universität wien

MASTERARBEIT / MASTER'S THESIS

Titel der Masterarbeit / Title of the Master's Thesis

„Multi-luciferase assay based characterization of geneticin-enriched transduced cells "

verfasst von / submitted by

Julia Moldaschl, BSc

angestrebter akademischer Grad / in partial fulfilment of the requirements for the degree of

Magistra pharmaciae (Mag.pharm.)

Wien, 2021 / Vienna, 2021

Studienkennzahl lt. Studienblatt / degree programme as it appears on the student records sheet:	UA 066 605
Studienrichtung lt. Studienblatt / degree programme as it appears on the student record sheet:	Masterstudium Pharmazie
Betreut von / Supervisor:	Univ.-Prof. Dipl. Ing. Dr. Manfred Ogris
Mitbetreut von / Co-Supervisor:	Dr. Haider Sami

ACKNOWLEDGEMENT/ DANKSAGUNG

Zuallererst möchte ich mich ganz herzlich bei Herrn Professor Manfred Ogris bedanken. Einerseits natürlich dafür, dass er mir die großartige Chance gegeben hat, meine Masterarbeit am „Laboratory of Macromolecular Cancer Therapeutics“ (MMCT) zu absolvieren und es mir somit ermöglicht hat, meine ersten Erfahrungen in der pharmazeutischen Forschung zu sammeln. Andererseits auch für die Betreuung meiner Bachelorarbeit und die durchgehende Unterstützung, die er mir in den letzten Jahren mit ganz viel Empathie entgegengebracht hat.

Ein besonders großes Dankeschön möchte ich an meinen Betreuer Dr. Haider Sami richten, der mir während der gesamten Zeit im Labor sowohl fachlich kompetent als auch persönlich beigestanden ist. Danke für das entgegengebrachte Vertrauen, die Motivation, Geduld und besonders dafür, ein Mentor für mich zu sein.

Weiters möchte ich mich beim gesamten MMCT-Team – Simon, Silvia, Fatih und Susi – bedanken, dass ich mit jedem Problem zu ihnen kommen konnte und sie immer ein verständnisvolles offenes Ohr für mich hatten, ihr seid großartig. Danke Dir, Steffi, für die schönen Gespräche und die tolle gemeinsame Zeit, die ich mit Dir in der „neighborhood“ verbringen durfte. Ich hätte mir keine bessere Kollegin wünschen können.

Besonders bedanken möchte ich mich an dieser Stelle bei Dominik. Danke, dass Du mir Tag und Nacht beistehst, mir den Rücken freihältst, meine Laune nicht nur vor Prüfungen hebst, mich motivierst und dabei unterstützt, meine Träume wahr zu machen. Danke, dass Du an meiner Seite bist.

Ganz großer Dank gebührt meiner lieben Familie und insbesondere meinen Eltern, die mir das Studium nicht nur ermöglicht haben, sondern mich auch grenzenlos unterstützen, an mich glauben und mir unendlich viel Verständnis entgegenbringen. DANKE.

Table of Content

1. Abstract

The formation of cancer is a process involving multiple parameters. In particular, mutated or dysregulated signal transduction pathways and cancer initiating stem cells play a key role in cancer progression and reduced responsiveness to chemotherapeutics. Investigations of the interplay of these substantial pathways offer a promising approach for the development of novel therapeutics for cancer treatment. Placed in this context, the signal transduction pathways Sonic Hedgehog, Notch and Wnt are quite important for their participation in tumorigenesis. Multiplexing applied within in-vitro assays and the use of multi-luciferase reporter plasmids may act as important methods for simultaneously examining the activity and cross-talk of the mentioned pathways in cancerous cells.

The focus of this thesis is on characterization of human embryonic kidney cells (HEK293T) stably transduced with the multi-luciferase reporter plasmid “3P-Luc” i.e. HEK293T 3P-Luc cells. These cells possess the 3P-Luc DNA, which encodes for three different luciferases, namely Firefly luciferase, Gaussia luciferase and NanoLuc. These are expressed under the control of promoter elements responsive to the Sonic Hedgehog, Notch and Wnt pathway, respectively. This enables studying activity of all three specific networks simultaneously. 3P-Luc transduced and geneticin-enriched HEK293T cells were analyzed for basal pathway activity by employing the Multi-Luc/BCA assay. This is a multiplexing experiment combining three different luciferase assays and one BCA assay for protein normalization. HEK293T 3P-Luc cells were also characterized for green fluorescent protein (EGFP) expression by flow cytometry studies as the 3P-Luc element also contains the EGFP gene under constitutive expression. In addition, nanocarrier based transfections with pathway inducer plasmids were performed in HEK293T 3P-Luc cells to check the responsiveness of these cells for pathway modulators.

2. Zusammenfassung

Die Entstehung von Krebs ist ein Prozess, der zahlreiche Parameter umfasst. Insbesondere mutierte oder fehlregulierte Signaltransduktionswege und sogenannte cancer initiating stem cells (CSC) spielen eine Schlüsselrolle in der Tumorprogression und der verminderten Ansprechbarkeit auf Chemotherapeutika. Untersuchungen des Zusammenspiels dieser bedeutenden Signalwege stellen einen vielversprechenden Ansatz für die Entwicklung neuer Wirkstoffe für die Krebstherapie dar. In diesem Kontext kommt den Signaltransduktionswegen Sonic Hedgehog, Notch und Wnt besondere Bedeutung an der Beteiligung der Krebsentstehung zu. Multiplexing in in-vitro-Versuchen und die Anwendung multipler Luciferase-Reporterplasmide können wichtige Instrumente für simultane Untersuchungen der Aktivitäten und Verstrickungen der erwähnten Signalwege in kanzerösen Zellen sein. Der Fokus dieser Arbeit liegt auf der Charakterisierung humanen embryonaler Nierenzellen (HEK293T), welche stabil mit dem multiplem Luciferase-Reporterplasmid, „3P-Luc“, transduziert sind, genannt HEK293T 3P-Luc Zellen. Diese Zellen besitzen ein 3P-Luc DNA Element, welches für drei verschiedene Luciferasen codiert, namentlich Firefly Luciferase, Gaussia Luciferase and NanoLuc. Diese werden unter der Kontrolle von Promoterelementen exprimiert, welche jeweils von den Signalwegen Sonic Hedgehog, Notch und Wnt aktiviert werden. Das ermöglicht die simultane Untersuchung der Aktivität aller drei Signalwege. Mit dem 3P-Luc Plasmid transduzierte und mit Geneticin angereicherte HEK293T Zellen wurden hinsichtlich ihrer basalen Signalwegeaktivität mittels Multi-Luc/BCA Assay analysiert. Dies ist ein Multiplex-Experiment, welches drei verschiedene Assays basierend auf Luciferasen und einen BCA Assay für die Proteinnormierung kombiniert. HEK293T 3P-Luc Zellen wurden auch hinsichtlich ihrer EGPF-positiven Zellen mittels Durchflusszytometrie charakterisiert, da das 3P-Luc DNA-Element das Gen für grün fluoreszierendes Protein (EGFP) unter konstitutiver Expression enthält. Zusätzlich wurden Nanocarrier-basierte Transfektionen mit Signalweg-induzierenden Plasmiden in HEK293T 3P-Luc Zellen durchgeführt, um die Ansprechbarkeit dieser Zellen hinsichtlich Signalweg-Modulatoren zu überprüfen.

3. Aim of the Thesis

This thesis intends to use a multi-luciferase assay combined with protein normalization (Multi-Luc/BCA assay) for characterization of geneticin-enriched 3P-Luc transduced HEK293T cells for estimation of activity of multiple signal transduction pathways: Sonic Hedgehog, Notch and Wnt. Towards this, following two sub-goals were defined:

1. Investigate Hedgehog, Notch and Wnt activity in HEK293T 3P-Luc cells after two different durations of growth and comparing two different lysis methods – one with scratching and the other one without scratching. Multi-Luc/BCA assay involves detection of Hedgehog pathway activity via firefly luciferase assay, Notch pathway activity via Gaussia luciferase assay and Wnt pathway activity via NanoLuc assay. Furthermore, conducting a BCA assay for protein estimation and performing all four assays combined in one run, in the frame of multiplexing. HEK293T 3P-Luc cells are also characterized for EGFP-positive cells by widefield fluorescence microscopy and flow cytometry measurements.

2. Characterizing responsiveness of HEK293T 3P-Luc for pathway induction by respective inducer plasmids for all three signaling pathways. On this account, performing linear polyethylenimine (LPEI) nanocarrier based transfections with polyplexes containing various inducer plasmids, namely pAd (Wnt pathway activity inducer), phGli1 (Hedgehog pathway activity inducer), phICN1 (Notch pathway activity inducer), and pUC19 (control plasmid).

4. Introduction

4.1. Signaling Pathways Involved in Cancer

Inherited or spontaneously arisen genetic or epigenetic alterations in tumor cells are usually considered as the main cause for the development of cancer. As a selective benefit for tumor cells, those alterations lead to overproliferation and escape from control mechanisms that suppress the survival and invasion of cancerous cells in other tissues. Frequently, components of cellular signal transduction pathways mainly controlling the cell growth, cell death and cell fate are affected by those mutations and, hence, dysregulated. In this state and placed in the context of deformation of comprehensive signaling networks, they are playing a pivotal role in terms of cancer progression caused by resistance to apoptosis and cell death in general. Furthermore, they are essential for changes in the tumor microenvironment, genetic instability, induction of angiogenesis, increased migratory capacity and inflammation. (Sever & Brugge, 2015)

This thesis surveys the activity of the developmental signaling pathways Sonic Hedgehog, Notch and Wnt in HEK293T cells. All three pathways are ancient conserved signaling pathways, regulating organ development and homeostasis during embryonic development in mammals. (Braune & Lendahl, 2016)

According to various studies, embryogenesis and tumorigenesis have a lot in common, since both processes are based on cell progression, differentiation and migration. Thus, the three vital signal transduction pathways, on which the thesis focuses, are not only operators in embryogenesis, but also key regulators in tumorigenesis when the pathways are modulated or mutated. Particularly, the mentioned pathways are closely associated with the control of cancer initiating stem cells (CSC), which are primarily responsible for tumor relapse after a preceding cancer therapy. (Carballo, Honorato, de Lopes & Spohr, 2018)

4.1.1. Sonic Hedgehog Pathway

The Hedgehog signal transduction pathway plays a central role in embryogenesis – as described before – and is mainly inactivated after birth. However, for some exceptions it can be reactivated in a healthy adult organism. The pathway has, for instance, the responsibility for the maintenance of somatic lung-, mammary-, skin- and erythropoietic stem cells, as well as pluripotent cells. In addition, the Hedgehog pathway is linked to the regeneration of prostate epithelium, lung epithelium and exocrine pancreas cells. (Carballo, Honorato, de Lopes & Spohr, 2018)

Apart from these tissues, the pathway can be found solely in primary cilia (PC), small organelles bound on the cell surface and able to receive mechanical, thermal and chemical signals. The Hedgehog protein family consists of three members: Sonic Hedgehog (Shh), Indian Hedgehog (Ihh) and Desert Hedgehog (Dhh). While Shh has the highest activity and a crucial function for cell type specification in the nervous system and for limbs patterning, Ihh plays an important role in skeletal development and Dhh is associated with the gonads. Shh signaling can be either autocrine or paracrine. The activation of the pathway can either occur non-canonical (operation of activation downstream of the Smoothened receptor) (Smo) or canonical (ligand-dependent interaction or receptor-induced signaling), in which this thesis is mainly interested. (Skoda, et al., 2018)

In the absence of the Shh ligand, the transmembrane protein Ptch1 inhibits the translocation of Smo, a G protein-coupled receptor protein, into the PC and therefore represses its activity. The Suppressor of fused protein (Sufu), a negative regulator of the Shh pathway, keeps binding the Gli transcription factors, prevents their translocation into the nucleus and consequently the downstream transcription.

In the canonical activated version of the pathway, the Shh ligand (a glycoprotein) interacts with Ptch1 and inactivates it, which leads to the degradation of Ptch1. Smo is no longer blocked by Ptch1, moves into the ciliar membrane and accumulates in the PC. There it initiates the downstream cascade by employing protein complex consisting of kinesin protein (Kif7), (Sufu), and Gli. Induced by Smo, Sufu releases the Gli family that

subsequently translocates in the nucleus and starts the transcription of the target genes, implying Ptch1 and Gli1, each with a positive and a negative feedback loop (Figure 1). (Carballo, Honorato, de Lopes & Spohr, 2018)

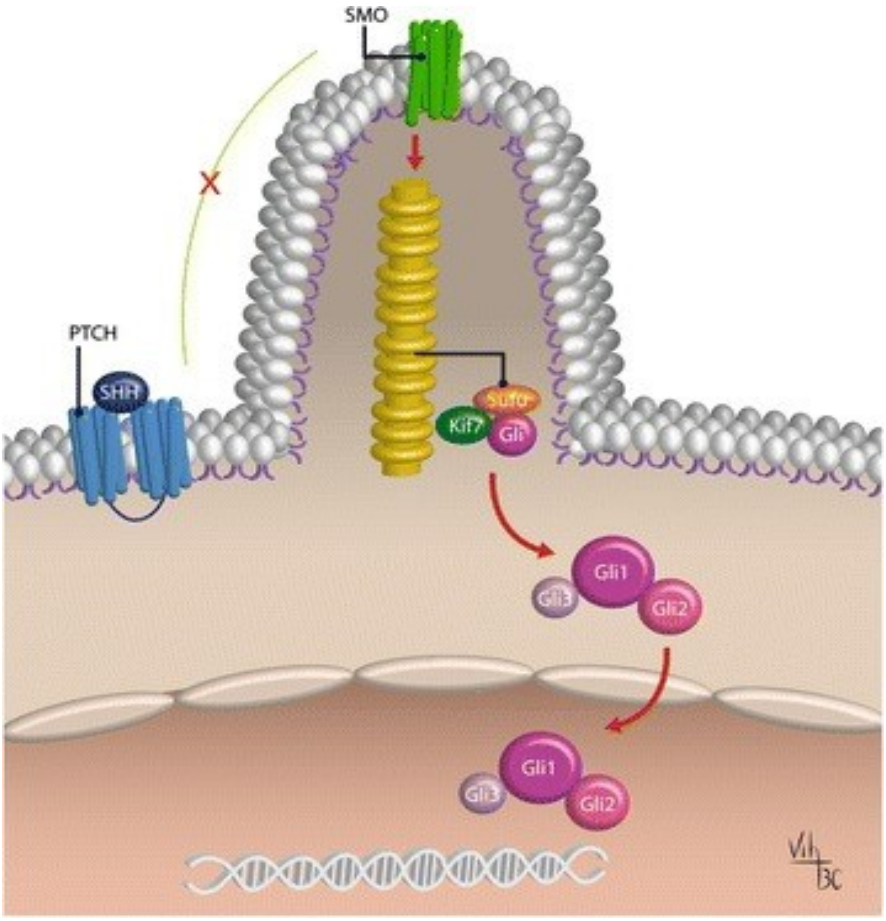

Figure 1: Schematic display of canonical activation of the Hedgehog signaling in primary cilia. (Figure from Carballo, Honorato, de Lopes & Spohr, 2018).
The Shh ligand (SHH) binds to Ptch1 (PTCH), followed by the activation of Smo (SMO) and the induction of the Gli downstream cascade, resulting in the activation of the target genes.

Hence, either the Gli activator (GliA) or the Gli repressor (GliR) are built to control the transcriptional activity of the Shh pathway, besides Sufu and Ptch1 (Skoda, et al., 2018). Studies reveal that mutations in the last two mentioned negative regulators are associated with the development of cancer; even the defect of Sufu is sufficient for activating the Shh pathway without the need for the receptor.

Another interesting issue is the crosstalk between Shh and other pathways which has the potential to influence the activity of the involved pathways in a positive or negative way. All those interacting pathways (TGF-β, EGFR, and Wnt) play a pivotal role during embryonic development and tumorigenesis, similar to Shh. The interplay with the Wnt signaling pathway, for instance, can occur in two different ways. The first option is Gli1 and Gli2, which are blocking Wnt ligands and/or the receptor by expressing the secreted frizzled related protein-1 (sFRP-1). In the second interacting way, GSK3β phosphorylates Sufu resulting in its separation, which leads to an increased activity of the Shh pathway. According to several studies, the interference between Shh and those pathways is crucial for the maintenance of CSCs. Their existence in a tumor bulk is mainly responsible for initiation, preservation and radio- and chemoresistance of malignant tumors as well as for their recurrence, which makes these tumors difficult to treat. Shh is associated with this process as it is upregulated in CSCs. Researchers assume that the Gli1 expression plays the major role in the chemoresistance in gliomas and that their overexpression leads to tumor recurrence. Therefore, the Shh pathway inhibition is supposed to increase the responsiveness to chemotherapy by down-regulating several genes associated with cell survival, apoptosis and multi-drug resistance. (Carballo, Honorato, de Lopes & Spohr, 2018)

4.1.1.1. Induction of the Hedgehog Pathway by Plasmid Transfection with phGli1

To validate the responsiveness of the Hedgehog pathway for pathway modulators, the cells in question are transfected with inducer plasmids containing pathway-activating genes. After a defined incubation time, the addressed signal pathway is expected to show a response in case of a successful induction, detectable in a higher luciferase activity. In this work, the inducer plasmid hGli flag 3x, in short “phGli1” was chosen for Hedgehog pathway induction.

After their binding to promotors, Gli transcription factors are responsible for the initiation of expressing Hedgehog target genes. For constructing the plasmid-based inducer for the Hedgehog pathway, a human Gli1 gene was cloned into a C-terminal p3xFLAG-CMV14 plasmid, resulting in phGli, as displayed in Figure 2 (Addgene).

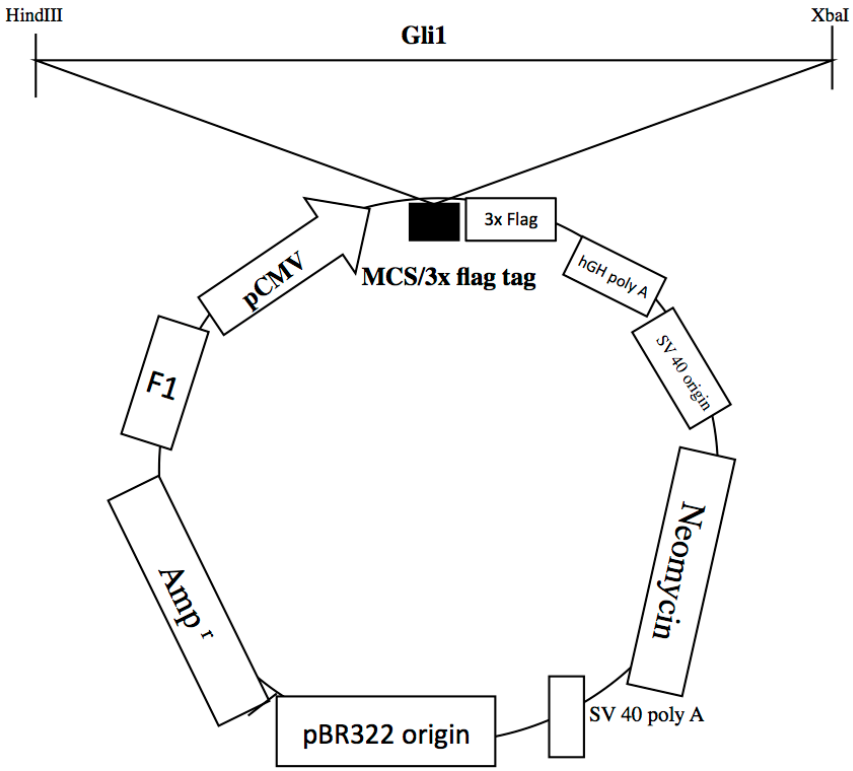

Figure 2: Map of the plasmid-based inducer phGli1 (Addgene plasmid #84922). (Figure from Addgene).

4.1.2. Notch Pathway

The Notch signaling pathway can be found in most of all multicellular organism and further in the majority of all cell types and is responsible for a great part of the embryonic development. In contrast to the Sonic Hedgehog pathway or the Wnt pathway, the Notch signal cascade is based on cell-cell communication, meaning that the extracellular ligand of one cell interacts with the transmembrane receptor of the adjacent cell. (Siebel & Lendahl, 2017)

The Notch signal cascade plays a key role in the main developmental processes of organs and tissues. On the one hand, it is able to inhibit cell differentiation and therefore provides a broad array of stem cells. On the other hand, it ensures the balance between two available potentially differentiated cell fates as an outcome for a stem cell.

The connection between Notch signaling and tumorigenesis hides a high level of complexity. Although mutations of the Notch pathway are only rarely involved in tumor development, there are some exemptions, for instance acute lymphoblastic leukemia

(T-ALL), small cell lung cancer (SCLC), non-small cell lung cancer (NSCLC) and skin cancer. Depending on the tumor type, the mutations of components of the Notch pathway are either gain-of-function mutations (Notch acts as an oncogene) or loss-of-functions ones (Notch serves as a tumor suppressor gene). More prevalent in disease and tumor events than mutations in the Notch pathway is the dysregulation of the Notch downstream signaling. The particularly pronounced dosage-sensitivity of the Notch signal is directly associated with this process. The right level of Notch signaling is crucial for the normal cell differentiation process, whereas a dysregulated signal may cause various diseases. For instance, a hyperactivated Notch signaling is linked with T-cell lymphoblastic leukemia (T-ALL), non-small cell lung cancer (NSCLC), breast cancer and prostate cancer. In contrast, in skin cancer, small cell lung cancer (SCLC), spondylocostal dysostosis and in various myeloproliferative disorders a hypoactivated Notch signaling was detected.

Despite the simple molecular architecture of the Notch signaling pathway, a quite versatile signaling output resulting in regulating cell fate in a broad array of cell types can occur. This diversity is not only remarkable, but has to be seen also as a hallmark of this signal transduction pathway. There are multiple potential explanations for this outstanding downstream diversity. At first, there are four different Notch receptors (Notch 1-4) and five different ligands, enabling a unique signaling output for each ligand-receptor pairing. Furthermore, different type-specific posttranslational modifications of Notch receptors, such as phosphorylation, acetylation, hydroxylation, ubiquitylation, and methylation, also increase this diversity.

When a transmembrane ligand of the Delta-like (DLL1, 3 and 4) or Jagged (Jagged1 and 2) protein family of a neighboring cell binds to a Notch receptor, a cascade of proteolytical cleavages of the Notch receptor starts. This process ends with the final cleavage – operated by the γ-secretase complex – and leads to the liberation of the Notch intracellular domain (Notch ICD or ICN). This domain translocates to the nucleus, where it generates a transcriptional complex together with the DNA binding protein CSL (CBF1, Suppressor of Hairless, Lag1; also called RBP-Jk), Mastermind-like protein (MAML), and transcriptional co-activators. This nuclear complex dictates the Notch downstream gene expression (Figure 3). (Braune & Lendahl, 2016)

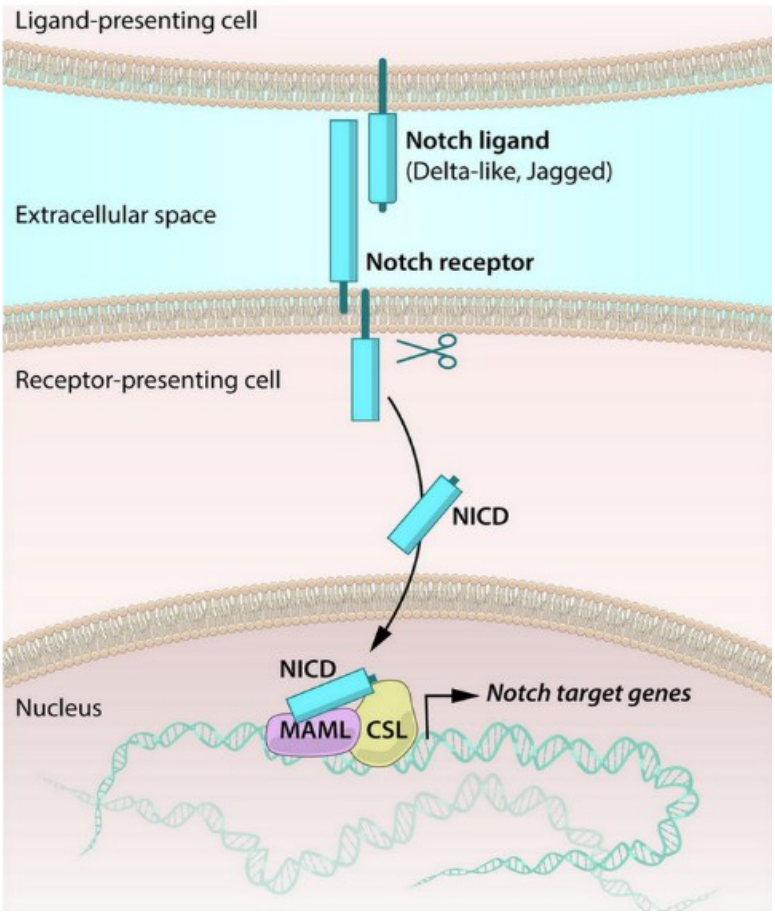

Figure 3: Schematic overview of the Notch signaling pathway. (Figure from Braune & Lendahl, 2016). The interaction of the Notch ligand with the Notch receptor of a neighboring cell initiates a series of cleavage processes of the Notch receptor. As the last step, the Notch ICD (NICD) is released and translocates into the nucleus, where it forms a complex with CSL (RBP-Jk) and Mastermind-like protein (MAML) promoting the expression of target genes.

4.1.2.1. Induction of the Notch Pathway by Plasmid Transfection with phICN1

In order to characterize the specificity of the Notch pathway initiation, a plasmid-based inducer was applied. After transfecting the cells in question with the inducer plasmids, the respective induced pathway is supposed to show an increased activity determined by measuring the luminescence emitted. For this thesis, the inducer plasmid EF.hICN1, also called “phICN1” was utilized for this approach, as displayed in Figure 4 (Maier, et al., 2019). ICN plays a pivotal role in the downstream of Notch effector genes, as described above.

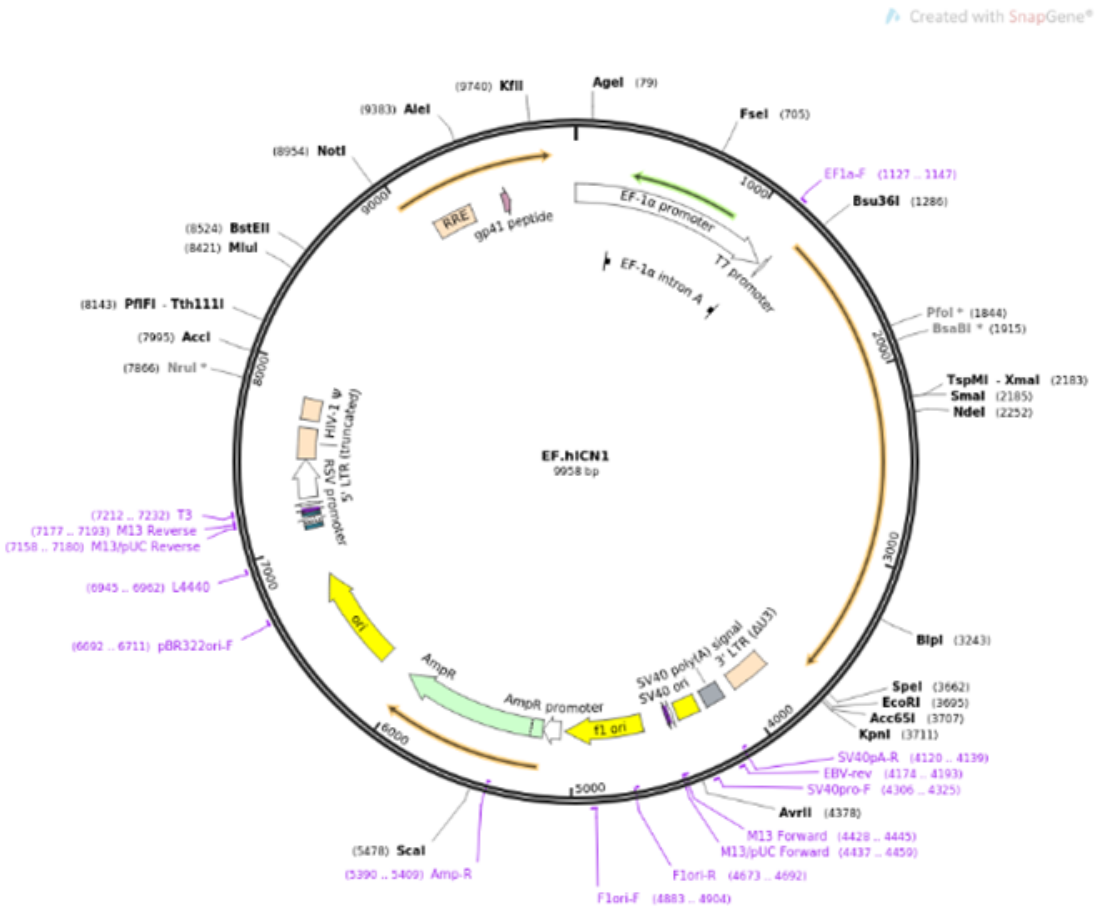

Figure 4: Map of the inducer plasmid phICN1 (Addgene plasmid #113715). (Figure from Maier, et al., 2019).

4.1.3. Wnt Pathway

Like the Hedgehog and the Notch pathway, the Wnt signaling pathway is an evolutionary conserved pathway in metazoan animals. It holds the control over essential aspects of for instance cell migration, neural patterning, primary axis formation and tissue homeostasis as well as over organogenesis during embryogenic development. Consequently, deregulated Wnt pathways may cause several pleiotropic pathologies including skeletal defects and human birth defect disorders, for instance Spina bifida. This pathway is essential in processes associated with tumorigenesis, as all control areas of this pathway have high relevance in tumor initiation, progression and metastasis.

Moreover, the discovery of the mouse proto-oncogene *Wnt1* indicates that the Wnt pathway may play a critical role in the development of cancer.

The name "Wnt" was derived from a fusion of *wingless* (the Drosophila segment polarity gene) and *integrated* or *int-1* (the name of the vertebrate homolog), as Wnt protein were initially identified as wingless protein in *Drosophila melanogaster*. The secreted Wnt proteins are cysteine rich molecules and underly 19 independent Wnt genes. Essential for the secretion of the proteins are post-translational modifications of the Wnt proteins in the endoplasmatic reticulum (ER), such as palmitoylation at a conserved serine residue. After this step, the Wnt molecules make use of palmitoylation dependent vesicular trafficking in cells resulting in the release into the extra-cellular environment, where they bind to active transmembrane ligand-activated receptors. Those Frizzled (Fzd) receptors possess an extracellular cysteine rich domain (CRD) at the N-terminal as well as at the intracellular C-terminal domain. This protein family consists of 10 different members, each of them favoring another Wnt ligand. By integrating into a hydrophobic chink in the CRD of the Fzd receptor, the unsaturated palmitoleic acid defines the specifity of the Wnt-Fzd binding. This binding is followed by dimerization/multimerization of the Fzd proteins with the Wnts. (Li, Ortiz & Kotula, 2020)

Wnt pathways can be divided into canonical (Wnt/β-catenin dependent pathway) and non-canonical ones (β-catenin dependent pathway), which can be further classified into the planar cell polarity pathways and the Wnt/Ca^{2+} pathways. (Komiya & Habas, 2008)

As this thesis focus on the Wnt/β-catenin dependent pathway, the function of this type will be described in detail as follows.

The canonical Wnt/β-catenin dependent pathway is characterized by the stabilization and nuclear translocation of β-catenin in the cell. In the inactivated state, when Wnt molecules are absent, β-catenin is a part and a stabilizer of a destruction complex. It consists of the scaffold proteins ACP and Axin, the Hippo signaling pathway components Yes-associated protein (YAP) as well as the transcription co-activator with the PDZ-binding motif (TAZ) and the kinases CK1α and GSK3α/β. Due to the destruction caused by complex-mediated phosphorylation of the conserved N-terminal serine/threonine

residues on β-catenin, E3-ubiquitin ligase $SCF^{\beta\text{-}TRCP}$ conducting ubiquitination is recruited and entails the following proteasome degradation (Figure 5 (a)).

In the activated state of the pathway, the binding of Wnt to the Fzd receptor and to its co-receptor low density lipoprotein receptor related protein 5/6 (LRP 5/6) leads to the dimerization of the receptor with LPR 5/6. This induces the recruitment of the cytoplasmatic Dishevelled protein (DVL) to the intracellular C-terminal domain of Fzd. By the interaction with Axin, DVL attracts the β-catenin destruction complex. CDK14-Cyclin Y, GSK3 and later the membrane anchored casein kinase 1γ phosphorylate the PPPSP motif of the LRP 5/6 intracellular tail. This process leads to β-catenin stabilization and, hence, accumulation as a result of the phosphorylated tail of LRP 5/6 blocking the GSK3 activity. Consequently, β-catenin translocates into the nucleus, where it acts as a key regulator for the activity of T-cell factor (TCF) lymphoid enhancer-binding factor (LEF) DNA binding proteins. TCF/LEF – repressors of Wnt responsive genes – bound to β-catenin lead to the transcription of Wnt responsive genes, and support proliferation and cell differentiation during tumorigenic and developmental processes. In parallel, the “Wnt-off” mechanism takes place: The GSK3 substrate phosphorylation and degradation are inhibited by the dissociation of the destruction complex, which enhances the effects of the β-catenin downstream transcriptional responses, as shown in Figure 5 (b). (Li, Ortiz & Kotula, 2020)

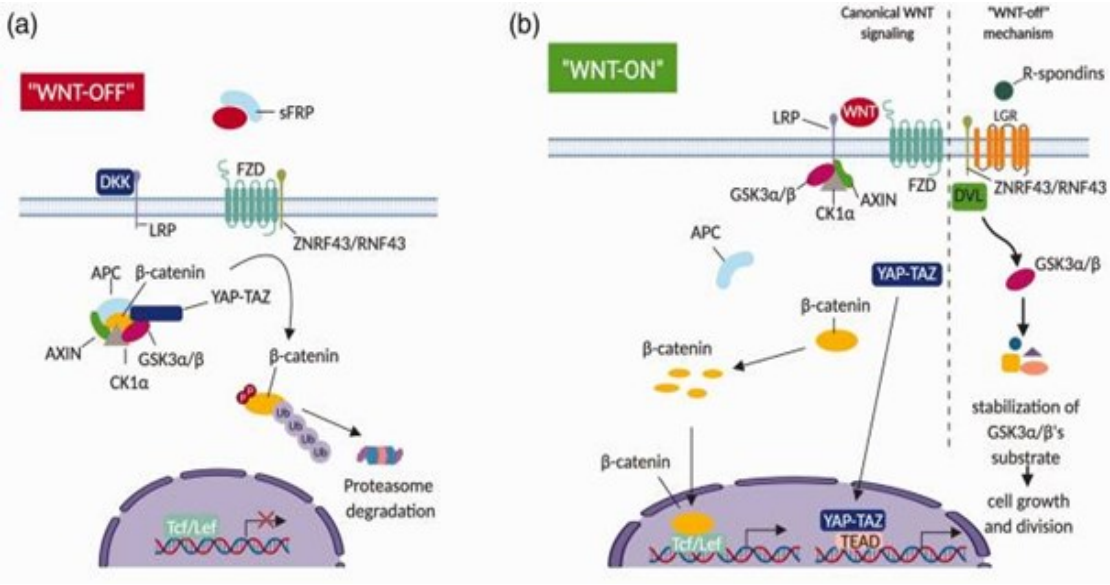

Figure 5: Schematic representation of the Wnt pathway in the inactivated state, in the absence of Wnt molecules (a) and the activated state, in the presence of Wnt molecules (b).
(Figure from Li, Ortiz & Kotula, 2020).

4.1.3.1. Induction of the Wnt Pathway by Plasmid Transfection with pAd-Wnt3a

To prove the specificity of the Wnt pathway activity, the cells in question are transduced with plasmids harboring pathway activating genes. After a defined incubation time, these cells are supposed to show a higher activity of the induced pathway. In this thesis, the inducer plasmid pAd-Wnt3a, in short “pWnt3a”, or “pAd” (Figure 6) was utilized for this investigation.

As mentioned above, the activation of the canonical Wnt signaling pathway depends on the binding of Wnt signal proteins (e.g. Wnt3a) to the Fzd receptor. For generating the adenoviral vector expressing the Wnt3a gene, the coding region of mouse Wnt3a was subcloned into the later vector backbone pAdTrack-CMV, which led to pAdTrack-Wnt3A, the plasmid used in the present thesis. (Luo, et al., 2004)

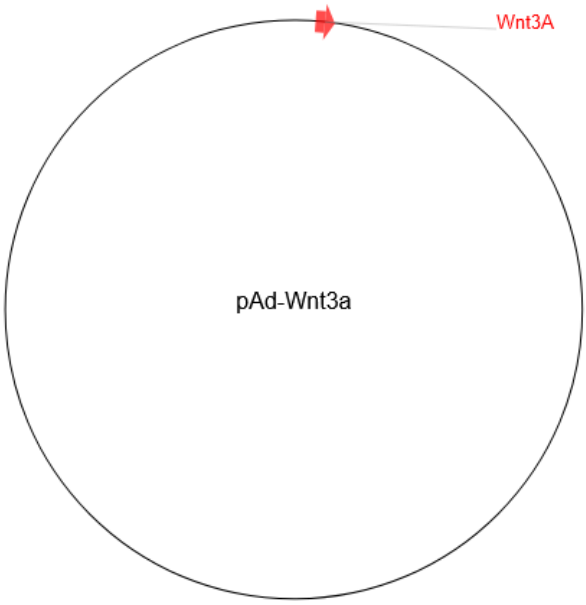

Figure 6: Map of the plasmid-based inducer pAd-Wnt3a (Addgene plasmid #12518). (Figure from Luo, et al., 2004)

4.2. Luciferase Based Reporters

Bioluminescence can be described as the emission of light from a living organism, which meets certain biological purposes. This phenomenon is widespread among a variety of terrestrial and aquatic organisms, including bacteria, insects, fungi and marine animals. It serves as a mechanism of self-defence, detecting food, interspecies communication and attracting prey (Lee, 2008). This biological light emission is caused by a chemical process in which it comes to an interaction between an enzyme – the luciferase – and a substrate compatible with the respective type of luciferase. In this case, the light actually poses the secondary product. The enzyme acts as a catalyzer of this reaction, generating most commonly yellow-green light (550–570 nm) with a peak at 562 nm or blue light, according to the luciferase gene used. (England, Ehlerding, & Cai, 2016)
This thereby generated so-called “cold light” is highly efficient due to its minimal energy loss compared to light produced from fire and connected with heat release (Thermo Fisher Scientific).

Beneficially, this light can be simply and properly detected and measured, amongst others due to the absence of background. Hence, bioluminescent systems are popular tools for many biomedical applications, for example for investigating gene regulation and cell signaling. (England, Ehlerding, & Cai, 2016)
Genetic reporters rightly became indispensable for biomedical research, drug development and biochemistry. Their working principle can be summarized as follows: The reporter gene is merged with the gene of interest, this chimeric sequence is cloned into an expression vector and together they are transferred into a suitable cell. Afterwards, the expression is then detectable by quantifying the light emission whose strength correlates with the intensity of the gene expression. The most common reporter systems are based on bioluminescence and provide high sensitivity. As a detection device of the emitted light signal, a luminometer equipped with a charge-coupled device (CCD) camera or a series of photomultipliers is used (Man, 2019). Ideally, the reporter gene provides a broad linear detection range. Other requirements for the reporter genes are the integrity of the normal physiology and health of the transfected

cell. On the one hand, bioluminescent reporter systems can act as markers for screening successfully transfected cells. They can serve as controls for standardizing transfection efficiencies or for studying regulation of gene expression. This can be used for instance for the investigation of the pathway activity. (Thermo Fisher Scientific)

4.2.1. Firefly Luciferase Based Reporter

As the most commonly used and best studied reporter enzyme, the Firefly luciferase originates from *Photinus pyralis*, the North American firefly, as shown in Figure 7 (Gibbons, Luker, & Luker, 2018).

Figure 7: A male *Photinus pyralis* flashing in flight.
(Figure from Beyond Your Back Door, 2020).

The Firefly luciferase is a 61kDa protein and has no need of subsequent processing for its activity. In the presence of ATP, molecular oxygen and magnesium, the Firefly luciferase (enzyme) catalyzes the oxidation of D-luciferin (substrate) to oxyluciferin. This results in a light emission with a wavelength of around 560 nm, whereas the light intensity directly correlates with the number of luciferase molecules (Figure 8). Since no endogenous luciferase activity exists in mammals, the Firefly luciferase is a really sensitive reporter, which poses a big benefit for its usage (Sigma Aldrich).

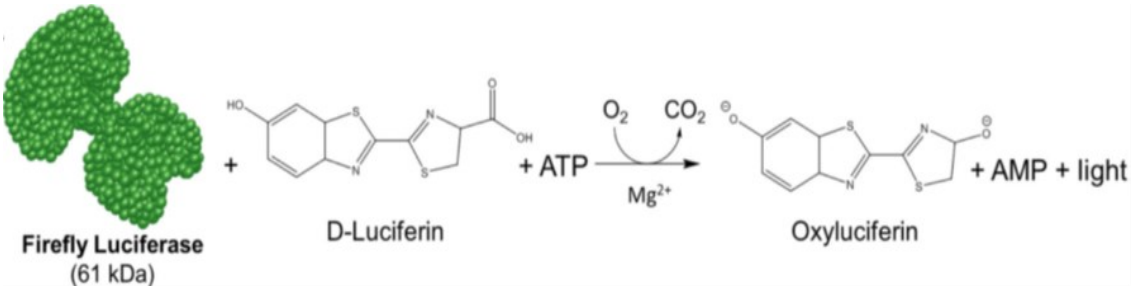

Figure 8: D-Luciferin undergoes an ATP-dependent oxidation to oxyluciferin with a light emission as a by-product. (Figure adapted from England, Ehlerding, & Cai, 2016).

A disadvantage of this reporter system is the fact that oxyluciferin is an intracellular protein, which means that it remains in the cytoplasm. Consequently, the lysis of the transfected cells can be necessary for the measurement. (The Y.O.R.F., 2007)

4.2.2. Gaussia Luciferase Based Reporter

Gaussia luciferase (a thermodynamically stable, 5-disulfide bridges containing enzyme) is originally secreted by *Gaussia princeps*, a marine copepod which is displayed in Figure 9. It lives in the dark of the deep ocean and its suddenly emitted light signal serves as a defence mechanism against dark-adapted predators. (The Y.O.R.F., 2007)

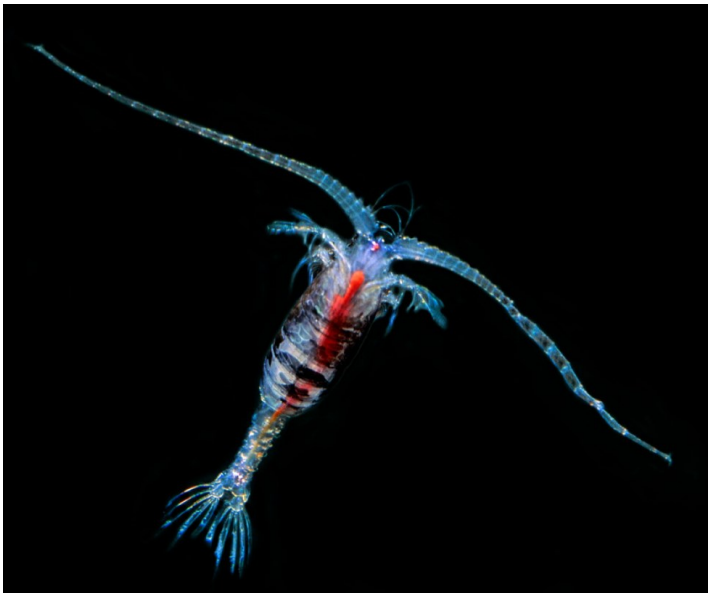

Figure 9: *Gaussia princeps* with its typical blue light output. (Figure from Wrobel).

In the presence of molecular oxygen and coelenterazine, Gaussia luciferase produces a strong ATP-independent blue burst of bioluminescence in the range of 475 nm. Beside this light emission, the end products of this oxidative carboxylation are coelenteramide and CO_2, as shown in Figure 10 (Yu, Laird, Prescher, & Thorpe, 2018).

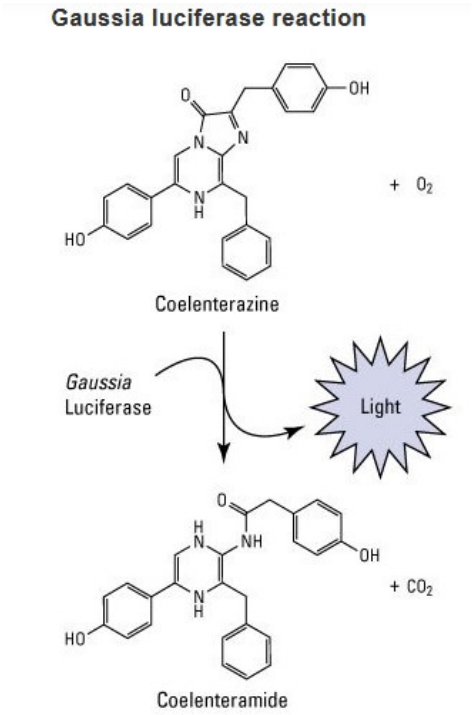

Figure 10: Gaussia luciferase catalyzes coelenterazine to coelenteramide with CO_2 and blue luminescence as secondary products. (Figure from Thermo Fisher Scientific).

As a big advantage, Gaussia luciferase is ATP-independent and has a small size of 20kDa (Thermo Fisher Scientific). Moreover, the protein is secreted into the supernatant – in contrast to measurable proteins of the Firefly luciferase and the NanoLuc reporter system. On the one hand, this renders the time-consuming step of lysing the transfected cells and allows live cell monitoring and, on the other hand, leads to very strong signals, when the supernatant of the cells in question is measured. (The Y.O.R.F., 2007)

More precisely, Gaussia luciferase provides a >1,000-fold higher bioluminescent signal intensity from live cells in the presence of the growth medium and a >100-fold higher intensity from cell lysates compared with Firefly luciferase expressed under the same conditions (Chopra, 2008). As a limitation, coelenterazine has shown to be less stable, less soluble, more toxic and more expensive than luciferin. Because of its secreted

product, the Gaussia luciferase reporter system is also limited in its potential applications. (England, Ehlerding, & Cai, 2016)

4.2.3. NanoLuc Based Reporter

As one of the latest commercially available luciferase enzymes, the NanoLuc luciferase (NanoLuc) is a synthetic version of the luciferase from the deep sea shrimp *Oplophorus gracilirostris* (Figure 11). As with *Gaussia princeps,* this marine organism naturally uses a sudden light signal for distraction of potential predators.

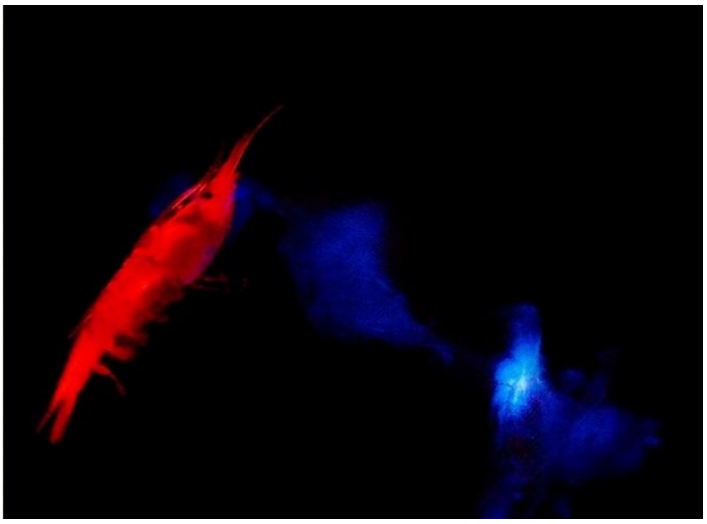

Figure 11: *Oplophorus gracilirostris* emitting its typical blue cloud of bioluminescent fluid as a defence mechanism. (Figure from JungleDragon).

NanoLuc offers certain advantages over established systems, for example over Firefly luciferase and Gaussia luciferase, as it is smaller sized (19kDa) and provides an enhanced stability as well as a >150-fold increase in luminescence. Moreover, the substrate of NanoLuc, furimazine, has an enhanced stability and a lower background activity, which enables the usage in a wide range of applications (Gibbons, Luker, & Luker, 2018). Despite the variety of benefits, it is also essential to demonstrate the potential limitations of this system.

Firstly, the emission wavelength of 460 nm is not ideal for in vivo investigations. Secondly, the reaction requires furimazine, which is not generically available and therefore its acquisition causes higher costs.

NanoLuc generates ATP-independent bioluminescence by reacting with furimazine in the presence of molecular oxygen which leads to the product furimamide, as it is displayed in Figure 12. As with oxyluciferin, furimamide is located in the cytoplasm, which requires the lysis of the transfected cells for enabling a measurement. (England, Ehlerding, & Cai, 2016)

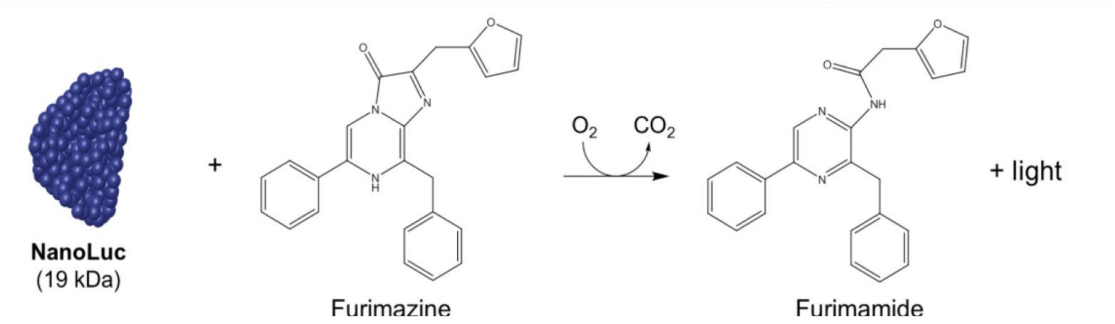

Figure 12: The reaction of NanoLuc with furimazine in the presence of molecular oxygen results in furimamide and a blue light emission. (Figure adapted from England, Ehlerding, & Cai, 2016).

4.3. Multiplexing Cellular Assays

The term “multiplexing” describes the approach of gaining more than one set of information from a single sample well. Due to the intricacy of cellular and biological systems, cellular (screening) assays based on solely single biological measurements are only capable of supplying a limited range of data and reach certain limitations, though. To give an example, independently conducted assays are not able to provide a proper control regarding their comparability, which hampers comparative studies across various experimental parameters. By simultaneously performing a multitude of read-outs from a single screening unit, multiplexing cell-based assays offer numerous benefits over single-read cellular assessments. For instance, multiplexing enables supplying more comprehensive and complete information about the event being measured. Therefore, it minimizes faulty interpretations and ambivalence of the data obtained. Besides, it increases the accuracy of the obtained results by putting the data into context. This can be accomplished by using the same variables for all assays performed on one sample by the mentioned technique and not introducing new variables through repetitive plating. Multiplexing also allows normalizing the measured data according to particular parameter, as relating the ratio of a detected event with the number of cells in the well of interest. Moreover, this method decreases the amount of work, the number of materials needed and therefore the general costs.
For making multiplexing even more applicable, the assays must meet certain requirements: The different assay chemistries must be compatible, the emitted signals of the multiple assays must be temporally or spectrally distinct and assays have to fit into the same well or must be separable in a simple way (signal output from cytoplasm and cell medium). As an example, a multiplexing cellular assay could be accomplished by both utilizing bioluminescent and fluorescent assays. (Hooper, 2011)

Due to their high sensitivity for reporting subtle changes in multiple signaling pathways, their flexibility and their cost-effectiveness, luciferase-based reporters emerged as an ideal tool for multiplexing, which demands reporters encompassing wide dynamic ranges. Luciferases provide several advantages over fluorescent proteins, like a broader

dynamic detection range, a higher sensitivity and the absence of auto-luminescence in mammalian cells. Each single luciferase has a unique emission spectrum enabling the simultaneous detection of multiple luciferases based on the distinguishability by emission spectra deconvolution. In addition, light emissions can also be differentiated by distinct substrates required, different cellular trafficking (cytoplasmatic vs. secreted) and enzyme kinetics (Maier, et al., 2019). The majority of the accomplished luciferase multiplex assays measures the light output of two or more luciferases sequentially in the same sample. In this case, the Firefly luciferase tracks the cellular signaling event in question, while the Renilla luciferase from *Renilla reniformis* acts as an internal control. Alternative luciferases for fulfilling this purpose are both the brighter NanoLuc and the Gaussia luciferase (Maier, et al., 2019). For a successful application in multiplex luciferase assaying, luciferases have to meet the following four criteria:

1) Luminescence quenching and the preference of utilization of a single substrate over another.

2) If the same substrates are preferred, minimal overlapping emission spectra distinguishable by emission filters and/or mathematical computation are obligatory.

3) Stability of the light emission signals during the experiment for gaining high quality reading.

4) A wide dynamic range of light emission for the ability to track even subtle changes in pathways' activity. (Sarrion-Perdigones, et al., 2019)

For gaining a facilitated practicability and minimizing possible experimental errors, the construction of a single plasmid, harboring all luciferase reporter units, is a promising option. It allows the detection of all pathways of interest by only one vector and therefore avoids multiple transfections of the cells in question. This approach emerged as a successful concept, as studies conducted by Maier, et al., 2019 and Sarrion-Perdigones, et al., 2019 show.

4.3.1. 3P-Luc Assay

In this work, the concept of multiplexing was employed for the accomplishment of the 3P-Luc assay, on which the main focus is placed. The triple-luciferase plasmid was designed by Maier, et al., 2019 and the Multi-Luc assay was optimized by Weiss, 2020, in order to characterize the cell line of interest for the developmental pathway activity of the three signaling pathways Sonic Hedgehog, Notch and Wnt, as mentioned above. As Gaussia luciferase is secreted in the cell medium, its emitted bioluminescence signal can be easily physically differentiated from the light outputs of Firefly luciferase and NanoLuc, which both remain in the cytoplasm. As mentioned above, the cells have to be lysed for the measurement of Firefly luciferase and NanoLuc.

The activities of all three pathways in one sample were measured and assessed. This was performed by sequentially measuring the bioluminescent light emission from the Firefly luciferase based reporter, the Gaussia luciferase based reporter and the NanoLuc based reporter. The Sonic Hedgehog pathway activity was determined by applying the Firefly Luc assay, while the Notch pathway was detected by employing the Gaussia Luc assay. In addition, the activity of the canonical Wnt pathway was quantified by using the NanoLuc assay. Further, all luciferase activities were normalized to the protein amount using the BCA assay and assessed. The detailed workflow and method of conducting the 3P-Luc assay can be found in *5.2.*.

This work benefits from the previous optimization of the multi-reporter luciferase assay as reported in Silvia Weiss's diploma thesis, which optimized the general workflow as well as the used amounts of reagents of the 3P-Luc assays conducted within this project. In both theses, the 3P-Luc assay was performed on HEK293T cells, but with one highly relevant difference. While Silvia Weiss worked with HEK293T wildtype (wt) cells, HEK293T cells used for this thesis were previously stably transduced with the 3P-Luc plasmid harboring the genes for Firefly luciferase, Gaussia luciferase and NanoLuc. As a consequence and benefit, there was no need for transient cell transfection with the 3P-Luc plasmid for each time conducting the 3P-Luc assay in this work, which had the big

advantage of avoiding errors done by transfection and saving a lot of materials and time.

4.3.1.1. 3P-Luc Plasmid

In this thesis, the following three luciferase based reporter plasmids were employed: TOP-NLuc (pMuLE_ENTR_TOP-NLuc1.1_L5-L4) for the Wnt pathway, GLI-FLuc (pMuLE_ENTR_12GLI-FLuc_R4-R3) for the Sonic Hedgehog pathway and CBF-GLuc (pMuLE_ENTR_CBF-GLuc_L3-L2) for the Notch pathway. Particular sections of these plasmids were taken for constructing a triple reporter plasmid: the 3P-Luc plasmid (pMuLE_EXPR_CMV-eGFP_TOP-NLuc1.1_GLI-FLuc_CBFGLuc), which is fully displayed in Figure 13. Additionally, the 3P-Luc plasmid contains a CMV-driven EGFP expression cassette for constitutive expression, emitting green fluorescence for fluorescence microscopy detection and future sorting purposes, as well as a PGK promoter-driven Neomycin resistance gene for enabling antibiotic-based selection.

The promotors of the three signaling pathways in question are integrated into the 3P-Luc plasmid and control the expression of their respective luciferase reporter genes (Wnt promoter: NanoLuc, Sonic Hedgehog promoter: Firefly luciferase, Notch promoter: Gaussia luciferase). Therefore, this multi-reporter plasmid enables the parallel measurement of all three pathways at once, which constitutes a big benefit. (Maier, et al., 2019)

The light emission produced by the luciferase reaction correlates with the amount of luciferase protein generated, which then is proportional to the respective pathway promotor activity driving the luciferase expression (Thermo Fisher Scientific).

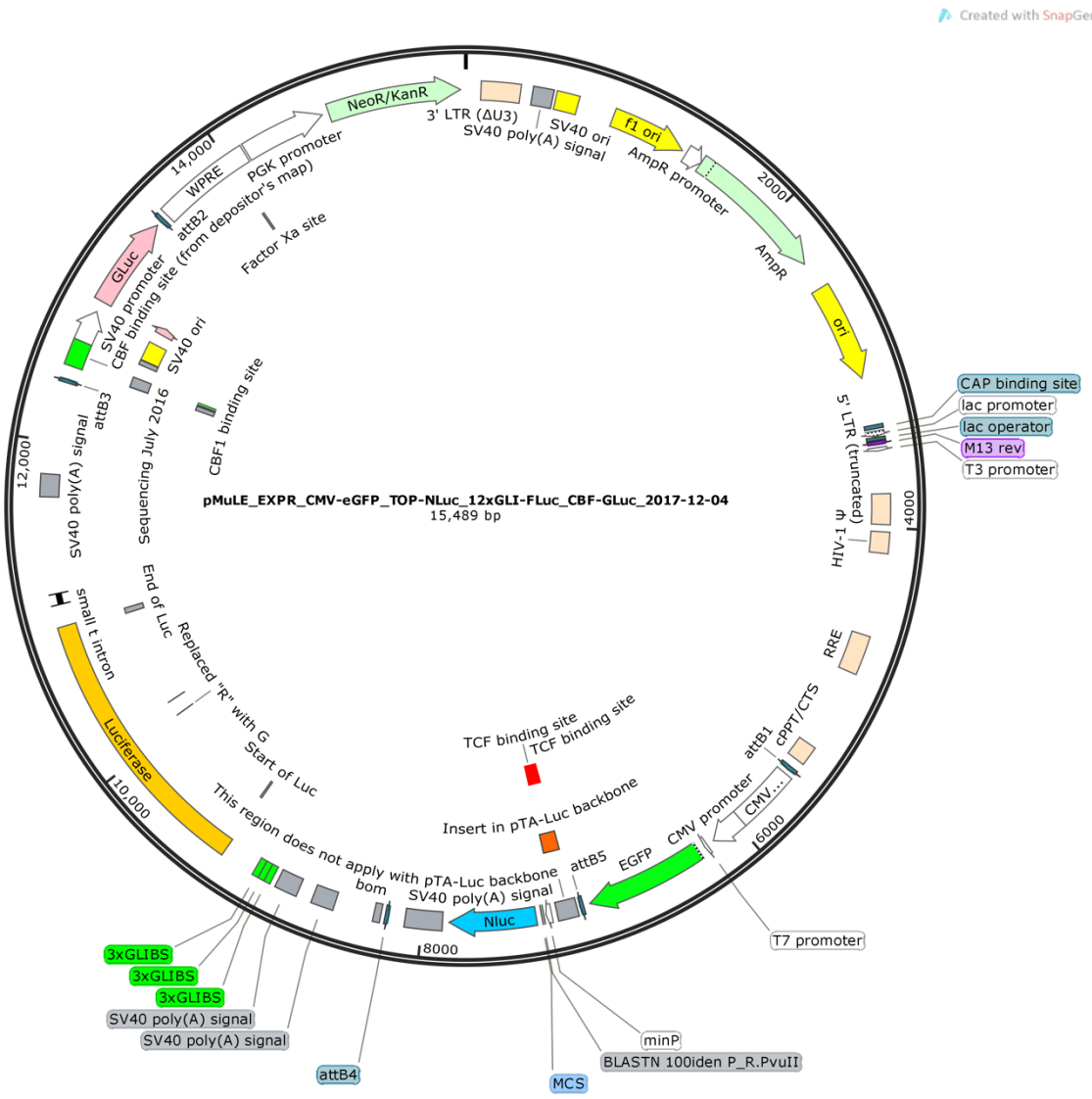

Figure 13: Map of the 3P-Luc plasmid. (Figure from Maier, et al., 2019).

Detailed map of the 3P-Luc plasmid, which harbors amongst others the Notch pathway promotor CBF-GLuc (rose), the Hedgehog pathway promotor GLI-FLuc

(orange), and the Wnt pathway promotor TOP-NLuc (light blue).

The plasmid additively contains a CMV-driven EGFP expression cassette for emitting green fluorescent signals for the purpose of future sorting, for instance by flow cytometry and a PGK promotor-driven Neomycin resistance gene for selection purpose.

4.3.1.2. Geneticin-Enriched HEK293T 3P-Luc

In the course of her doctoral thesis, Julia Maier stably transduced the HEK293T cells with the 3P-Luc multi-luciferase plasmid by using a lentivirus. Those non-sorted HEK293T 3P-Luc cells were then thawed and expanded until they could be handled at biological safety level 1. Further, they were selected by enrichment with Geneticin (G418) at a concentration of 1000 µg/ml in the course of Alison Camungol's diploma thesis. Due to their Neomycin resistance gene, which is harbored in the 3P-Luc plasmid, HEK293T 3P-Luc cells are suitable for selection through Geneticin, an aminoglycoside antibiotic similar in structure to Gentamicin (Sigma Aldrich). Alison Camungol brought them to the status where 20% of all the HEK293T cells carried the 3P-Luc plasmid. From this stage on, the cells were utilized for the experiments discussed in this thesis and further enriched with 1000 µg/ml Geneticin over multiple passages.

4.4. Cell Lysis

For successfully investigating the intricate network of intracellular processes, single-cell studies are indispensable. The method of cell lysis finds a broad application in the fields of biological and biomedical research. Therefore, it acts as the first step not only in protein extraction and purification, but also in cell fractionation and cell organelle isolation. Hence, numerous methods of cell lysis were developed in the course of time to meet different requirements. All methods have the constant aim of attaining the highest possible yield and purity of target molecules (proteins), subcellular structures or sample types (cells or tissue). In all cases, cell lysis intends to destruct the natural barrier of the target cell, which separates cell content from the environment. Bacteria and yeast possess cell walls which are composed of peptidoglycan or ß-glucan, respectively, and are additionally surrounded by an outer glycoprotein layer. Plant cell walls consist of multiple layers of cellulose, that leads to a higher effort needed for disrupting them. In contrast to these mentioned cell lines, bacterial cell walls are the easiest to lyse. The absence of an extracellular wall in animal cells makes them relatively simple to break as well.

The extracted protein can originate from natural sources, such as from mammalian cell cultures, tissues, bodily fluids or from overexpression in model systems. Hence, the sample preparation and the lysis technique cannot be universal. Highly relevant are also the cellular or subcellular location of the protein in question. In addition, the obtained protein yield depends on the downstream applications (eg. Western blotting, mass spectroscopy or reporter assays). In particular, the quality or physical form of the extracted protein must be taken into account. For instance, techniques like crystallography or the functional enzyme-linked immunosorbent assay (ELISA) require not only intact proteins, even functional activity or maintenance of their 3D structure is demanded. Another critical factor for the choice of the lysis technique is the compatibility with the experimental platform as, for instance, the capability of interlinking with capillaries for electrophoretic assays (Brown & Audet, 2008). Taken together, the technique of cell lysis in its diverse forms enables a multitude of

proteomic research methods and therefore emerged as a crucial instrument in modern natural sciences. (Promega)

Methods

Cell lysis can be roughly divided into two major categories: physical methods and reagent-based methods. Physical methods can be further sub-grouped into mechanical disruption, liquid homogenization, sonication, the freeze-thaw technique and manual grinding. Although physical cell lysis was the method of choice in the past for cell disruption and protein extraction, detergent-based lysis has become state of the art in recent times owing to its considerable advantages. Reagent-based solutions consisting of certain types and concentrations of detergents (with both lysing and solubilizing effects), buffers, salts and reducing agents were developed by empirical testing. (Thermo Fisher Scientific)

Physical Methods

As mentioned above, a wide variety of techniques for protein extraction by physical disruption were developed in the course of time. As one of them, mechanical disruption utilizes rotating blades to mill and disperse big pieces of tissue, for example liver or muscles. Usually, a Waring blender or a Polytron are applied for this purpose. While the Waring blender resembles a standard household blender, the Polytron works by drawing the tissue into a long, narrow shaft with rotational blades in it. To absorb a broad spectrum of volumes, the offered shafts vary in size.

The most commonly used option for lysing small volumes or cultured cells in a physical way is the liquid homogenization. It works by compelling the cell suspension through a narrow space, that leads to shearing the cell membranes. Devices either act as a Dounce Homogenizator (with a manually driven pestle), a Potter-Elvehjem Homogenizer (using a manually or mechanically driven pestle) or a French press, which forces the sample to a tiny hole in the press to exert high pressure on the cells to be lysed. Although the equipment for the French press is quite expensive, the method is most frequently used for lysing bacteria cells mechanically.

With the Sonication technique, cells, bacteria, spores, and finely diced tissue slices are agitated and lysed by applying pulsed, high frequency sound waves. The sound waves are generated by a sonicator, an apparatus with a vibrating probe immersed in the cell suspension. The energy generated from the probe creates microscopic bubbles that implode and lead to shock waves radiating through the sample.

The freeze-thaw technique is the fourth class of physical disruption of bacterial and mammalian cells. The methods rely on freezing the liquid cell sample in a dry ice/ethanol bath or freezer, followed by thawing it at 37°C or room temperature. The cells of interest enlarge and subsequently break because of ice crystals formed during the freezing process, followed by a shrinking process. By performing multiple freeze-thaw cycles successively, proper cell lysis can be achieved. Despite the slowness of the process, it is known as the most efficient method for liberating recombinant proteins enriched in the cytoplasm of bacteria.

Manual grinding is the most commonly applied method for lysing plant cells. The frozen plant tissue in liquid nitrogen is simply grinded and crushed by a mostar and a pestel. Considering the tensile strength of the plant cell wall consisting of cellulose and other polysaccharides, this procedure emerged as the most rapid and efficient way to release plant proteins and DNA.

In addition, several additives and agents for facilitating physical cell lysis are known. Cell disruption can be, for instance, encouraged by suspending the cell in a hypotonic buffer, which promotes cell bursting under physical disruption. Yeast and bacterial cell walls can be more easily broken by adding lysozymes (digesting the polysaccharides part of the cell wall) or glass beads, an additional crushing component. By adding DNase (25–50 µg/mL) along with RNase (50 µg/mL) to the samples, the viscosity caused by the release of nucleic acids, can be successfully decreased. As proteolysis may occur when cells are destructed, adding protease inhibitors to the lysing sample prevents this undesired process. (Thermo Fisher Scientific)

Passive Lysis Buffer (PLB) as Detergent-Based Method

Various cell lysis solutions exist, each optimized for the application on different species of organism and diverse cell and tissue types. Detergents, the main component of cell lysis solutions, destruct the cell membrane and wall surrounding the cell of interest by interrupting lipid–lipid, protein–protein as well as protein–lipid interactions and release proteins through solubilization. These amphipathic self-associating molecules consist of a polar hydrophilic “head” and a nonpolar hydrophobic “tail” and are grouped in ionic, nonionic and zwitterionic detergents, whereof their behaviour depends on. The milder and less denaturating nonionic and zwitterionic detergents are rather utilized for solubilizing membrane proteins for enzyme assays or immunoassays where it is critical to retain protein function and/or to preserve native protein–protein interactions. The application of ionic detergents for this approach is inappropriate because of their high solubilizing agents tending to denature proteins which results in the destruction of protein activity and function. The selection of the detergent depends on the sample type, the presence or absence of a cell wall and the downstream application. Parallel to the selection of an appropriate detergent, the choice of the buffer, salt concentration, pH value and temperature also has to be considered for a productive and successful protein extraction. (Thermo Fisher Scientific)

In this thesis, PLB was selected for disrupting the cells in question in a detergent-based way, as this cell lysis solution was developed for the rapid lysis of mammalian cells. By applying PLB, the cell lysis can be passively performed avoiding freeze-thaw cycles and when using sufficient reagent even without the need of scraping adherent cells. The cell lysis efficiency, however, depends on the cell type and needs to be evaluated especially when treating cells resistant to passive lysis buffers. A great advantage is the anti-foam agent that PLB contains. It avoids bubble formations, which may lead to instrument contamination and a less consistent detection of light output, that would influence the results in a negative way. Due to its minimal coelenterazine autoluminescence, PLB is the reagent of choice for applications including the coexpression of Firefly luciferase with a second or third reporter gene. (Promega)

In this work, PLB was applied in a multi-reporter assay including four different assays, which means the volume of the added reagent to the cells has to correlate with the required cell lysate amount for reading. PLB 5x was used in its diluted form with MilliQ water – as PLB 1x – and directly added to the cells in question. In previous multi-reporter assays (Weiss, 2020) 40 µl of PLB 1x were used, whereby it was necessary to scratch the lysed cells from the well plate after the disruption process. The same volume was used in this work in connection with the need for scratching the cells from the surface, directly compared with lysing the cells with 50 µl PLB 1x for the same incubation duration. By utilizing this higher amount, 10 µl more than required for reading the multi-reporter assay are used, which is considered to enhance the lysis efficiency and therefore ultimately avoid the necessity of scraping the solid components of the cell lysate from the well plate.

The common method of Multi-Luc/BCA assay reading, including scratching the lysed cells from the well-plate unfortunately comes along with certain problems originating in the technique of scratching, of which was taken notice in previously performed training experiments. Although scratching only poses a small part of the whole multi-reporter luciferase assay, it has the potential for influencing the resulting protein amounts tremendously. Due to the absence of a precise protocol defining this technique, scratching can be conducted in various ways concerning the duration, strength and the scraping pattern – strongly depending on the individual style of the executing person. Consequently, this technique includes a source of error and results obtained by different persons cannot be considered as properly comparable. Moreover, the well-plate may even break in case of scratching with too much power, which means the sample is lost and cannot be analyzed. Another limitation is the potential overspill of two wells in physical proximity, which may cause disproportionately high or low and ultimately wrong protein values. Unfortunately, this is only partly avoidable by covering the well-plate with the lid during the process of scratching. The most problematic aspect of scratching, though, is the high amount of cell lysate which gets lost during this process – resulting in an insufficient amount of cell lysate available for a further performance of the Firefly Luc and NanoLuc read-out.

Advantages and Disadvantages of Different Methods

The traditionally used physical method for cell lysis unfortunately comes with various disadvantages. To begin with, this technique tends to overheat the sample, resulting in protein denaturation and aggregation, which can be inhibited by pre-chilling the equipment and keeping the sample on ice continuously. Moreover, reproducibility may vary due to imprecise terminology used to describe sample handling. As an additional problem, cells breaking at different times during the lysis process cause an inconsistent viscosity of the medium and released subcellular structures that are exposed to ongoing disruptive forces. Furthermore, some physical lysis techniques involve costly equipment, like the French press or the sonicator, are impractical in use and not compatible with small volumes and high throughput.

The reagent-based cell lysis method, on the contrary, can be applied on small sample volumes, offers high reproducibility, is not only gentle, but also quick and leads to a high protein yield. To name the negative aspect, since high concentrations of salt and detergents pose a problem, this method is inappropriate for mass spectroscopy and furthermore, some elements of the detergents have to be removed for downstream analyses. (Thermo Fisher Scientific)

5. Materials and Methods

5.1. Equipment

List of equipment

- Biological safety cabinet (Thermo Fisher Scientific)
- Centrifuge (Thermo Fisher Scientific)
- Centrifuge tube 15ml (CT-15ml) (Starlab)
- Centrifuge tube 50ml (CT-50ml) (Starlab)
- Counting chamber (Neubauer-improved, Paul Marienfeld GmbH & Co.KG)
- Eppendorf tubes (Nerbe plus GmbH)
- Flow Cytometer (MACSQuant Analyzer 10, Miltenyi Biotec)
- Freezer (-20°C, -80°C) (Thermo Scientific)
- Incubator 37°C, 5% CO_2 (Thermo Fisher Scientific)
- Inverted microscopes (Motic, Olympus)
- Multichannel pipette (VWR)
- Multimode Microplate Reader (GloMax, Promega)
- Pipette boy (Integra)
- Pipette tips (Nerbe plus GmbH)
- Plate reader (Infinite M200 Pro, Tecan)
- Plate shaker (Eppendorf)
- Reagent reservoirs (Starlab)
- Refrigator (4°C) (Allectric)
- Serological pipettes 5ml, 10ml, 25ml (Sarstedt)
- TC flask T75, standard, vent. Cap (Sarstedt)
- Transparent 96-well flat-bottom microplate, sterile (Starlab)
- Vacuum aspiration system (Integra)
- Vortex mixer (Starlab)
- Water bath (VWR)
- White 96-well flat-bottom microplate, transparent bottom, sterile (Greiner)

List of reagents

- BCA Protein Assay Kit (Pierce, Thermo Fisher Scientific)
- Bovine serum albumin (BSA) 2mg/ml (Pierce, Thermo Fisher Scientific)
- Bovine serum albumin (BSA) powder (Sigma-Aldrich)
- Cell line: HEK293T wt, HEK293T 3P-Luc
- Coelenterazine
- Dulbecco's modified eagle's medium (DMEM) high glucose (Sigma-Aldrich)
- Dulbecco's phosphate buffered saline (DPBS) (Sigma-Aldrich)
- Ethylenediaminetetraacetic acid (EDTA) (Sigma)
- Fetal bovine serum (Biowest)
- Geneticin (G418) (InvivoGen)
- HEPES buffered glucose (HBG, 5% glucose w/v, 20mM HEPES pH 7.4), MMCT (University of Vienna)
- L-Glutamine 200mM (Sigma-Aldrich)
- Linear polyethylenimine (LPEI) 10kDa, MMCT (University of Vienna)
- Luciferase assay reagent buffer + luciferin (LBL)
- MilliQ-water (Sartorius)
- NaCl (Sigma-Aldrich)
- Nano-GloR Luciferase Assay Buffer + Substrate (Promega)
- pAd (pAd-Wnt3a was a gift from Tong-Chuan He (Addgene plasmid #12518))
- Passive Lysis Buffer 5x (PLB 5x) (Promega)
- Penicillin-Streptomycin (Sigma-Aldrich)
- phGli1 (hGli1 flag3x was a gift from Martin Fernandez-Zapico (Addgene plasmid #84922))
- phICN1 (EF.hICN1 was created in the MMCT (University of Vienna) (Addgene plasmid #113715)
- pUC19 (was a gift from Joachim Messing (Addgene plasmid #50005))
- Trizma R base (Sigma-Aldrich)
- Tryp-LE (Gibco, Thermo Fisher Scientific)

(This list was derived from Weiss, 2020 and adapted.)

5.2. Workflow for Multi-Reporter Luciferase Assay Read-Out

The main steps for studying the activity of signaling pathways via the Multi-Luc/BCA assay are cell seeding into a white 96-well plate on Day 1 and reading the luminescence signals after adding the substrate on Day 2 or Day 3 (24 hours respectively 48 hours after seeding), as shown in Figure 14.

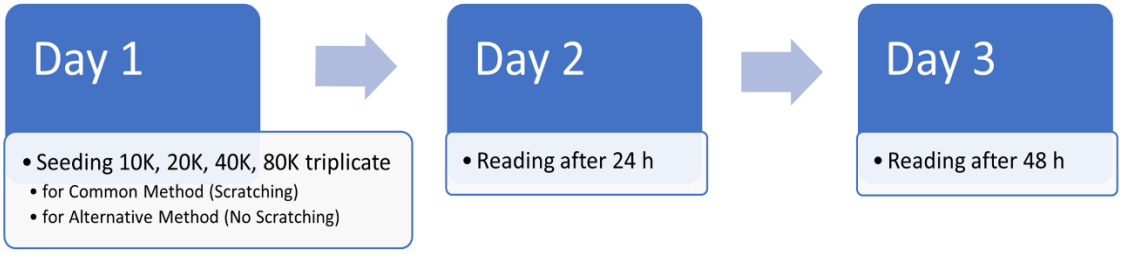

Figure 14: Workflow for the Multi-Luc/BCA assay.

This assay was carried out with both HEK293T 3P-Luc and HEK293T wt cells, whereas wt cells served as a control. The common method of the Multi-Luc/BCA assay (Weiss, 2020) was compared with an alternative method without scratching and only lysing, therefore cell seeding for both methods was done into the same plate, while two plates were seeded collectively for reading after 24 hours and 48 hours.

5.2.1. Cell Line for Studying Signaling Pathways

In the early 1970s, Human embryonic kidney (HEK) cells were isolated from an aborted human embryo and transfected with sheared adenovirus 5 (Ad5) DNA, resulting in a currently widespread expression tool – the HEK293 cell line. Incorporating Ad5 into chromosome 19 of the host genome leads to the ability of producing recombinant E1-deleted human adenoviral vectors, which are known as transcription incompetent. In other words, this modification lets this cell line arise to a highly efficient tool for generating high amounts of recombinant proteins from plasmid vectors carrying the CMV promoter region. HEK293T is a daughter cell line with incorporated SV40 large T antigen into the host genome. (Roberts, 2020)

As the second most widely used cell line, it provides numerous advantages. HEK293T is a hardened, rapidly dividing and semi-adherent cell line, culturable in suspension or as a monolayer, capable of generating large amounts of proteins and simple to transfect through various methods. However, as a human cell line, it faces the risk of contamination with human-specific viruses. Culturing HEK293T for a prolonged period of time results in health decline, which negatively impacts the growth rates and translation efficiency. HEK293T is not only extensively used as a transient expression system, but also popular and esteemed in stably transduced forms, as it is the case in the thesis at hand, to study a multitude of cell-biological questions (Thomas & Smart, 2005). Due to their wide range of benefits and their versatility, HEK293T cells are widely applied and indispensable in the fields of cancer research, neuropharmacology, cellular signal transduction studies and protein production. (Roberts, 2020)

As an immortalized embryonic cell line and due to its well comparable environment and properties to the one in and of dysregulated cancer stem cells, HEK293T emerged as an ideal tool for studying the three embryonic cancer signaling pathways of interest which are known to be overexpressed in this cell line (Takebe, et al., 2015).

For this thesis, the cells were cultured in DMEM (Dulbecco's Modified Eagle's Medium) with 10% fetal bovine serum (FBS), 2% L-Glutamine and 1% Penicillin/Streptomycin at 37 degrees Celsius and 5% CO_2.
HEK293T 3P-Luc cells were further enriched with 1000 µg/ml G418 and weekly characterized for their EGFP expression by fluorescence microscopy and finally by flow cytometry.

5.2.2. Cell Seeding

On the first day, both HEK293T wt and HEK293T 3P-Luc, which are kept in T-75 flasks, were taken out of the incubator and their medium was checked visually regarding the color as well as the turbidity. The cell confluency, which ideally has to be around 80%, was seen under the microscope. Furthermore, the cells were characterized for EGFP

expression by fluorescence microscopy. After transferring the flasks to the biological safety cabinet, the used medium was removed and the bottom of the flask was gently washed with 10 ml phosphate buffered saline (PBS). For detaching the cells from the surface, 1 ml Tryp-LE was added and the cells were stored in the incubator (37°C, 5% CO_2) for 4 minutes. As the next step, the cells were transferred into CT-15 tubes by using complete medium and centrifugating them for 5 minutes. After the supernatant was removed, the cell pellet was gently resuspended in 1 ml complete medium.

The cells were counted with the counting chamber and the respectively required volume of cell suspension was calculated to obtain a cell density of 10,000, 20,000, 40,000 or 80,000 cells per well. Initially, the calculated amount of complete medium was pipetted in triplicates into each well of two white 96-well plates with flat bottom for reading after 24 hours and 48 hours. HEK293T wt were seeded into the upper part of the plate and HEK293T 3P-Luc into the lower part. Both cell types were seeded twice on each plate for comparing the common method with the alternative method, as it is displayed in Figure 15.

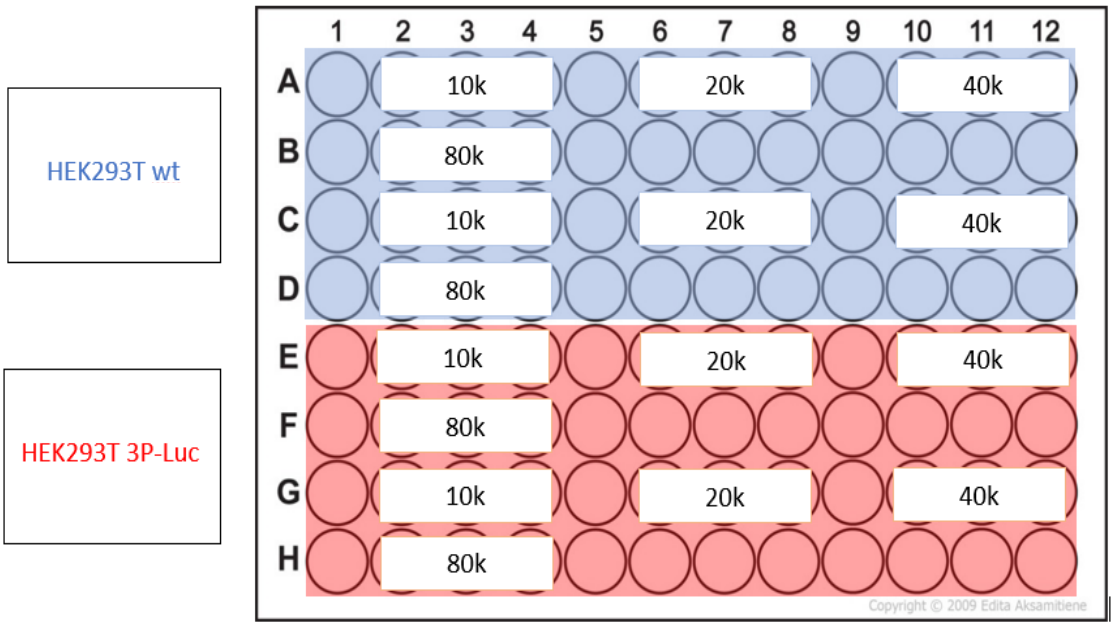

Figure 15: Schematic overview of 96-well plate showing the cell seeding plan, with HEK293T wt cells in the upper part and HEK293T 3P-Luc cells in the lower part of the plate.

As the next step, the dilution of the cell suspension was added into the wells, resulting in a total volume of 200 µl of cell suspension and medium in each well. The wells were checked under the microscope and both plates were put into the incubator for 24 hours respectively 48 hours.

5.2.3. Reading Multi-Luc/BCA Assay

Both the common method and the alternative method were applied on HEK293T 3P-Luc cells while HEK293T wt cells served as a control. While the common method was applied on the upper row of the respective cell type, the lower row of each cell type was reserved for the treatment with the alternative method without scratching (Figure 16).

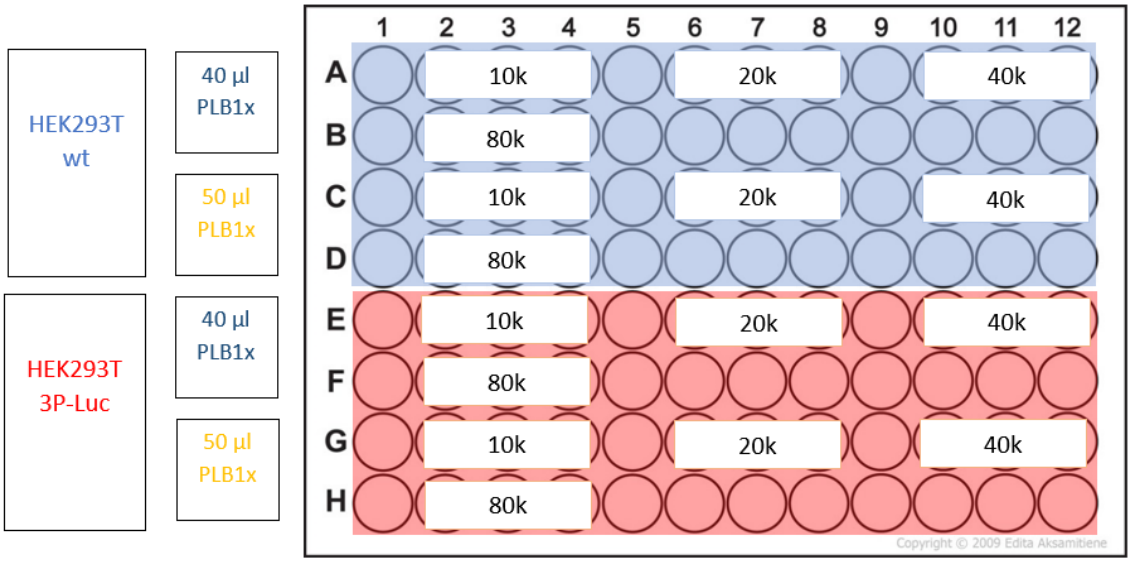

Figure 16: Schematic overview of the treatment strategy.

While the upper seeding row of each cell line was treated with 40 µl PLB 1x (common method), 50 µl PLB 1x were added into the lower seeding rows (alternative method).

5.2.3.1. Luciferase Assay

Common Method

After 24 hours respectively 48 hours, the respective plate (plate 1) was taken out of the incubator and visually checked under the microscope. The reading process of the Multi-Luc/BCA assay was performed according to the modified protocol by Silvia Weiss, described in her diploma thesis (Weiss, 2020). Protein amount via BCA assay, Firefly luciferase and NanoLuc were all read from the cell lysate, while Gaussia luciferase was read from the supernatant. The whole process is displayed in Figure 17.

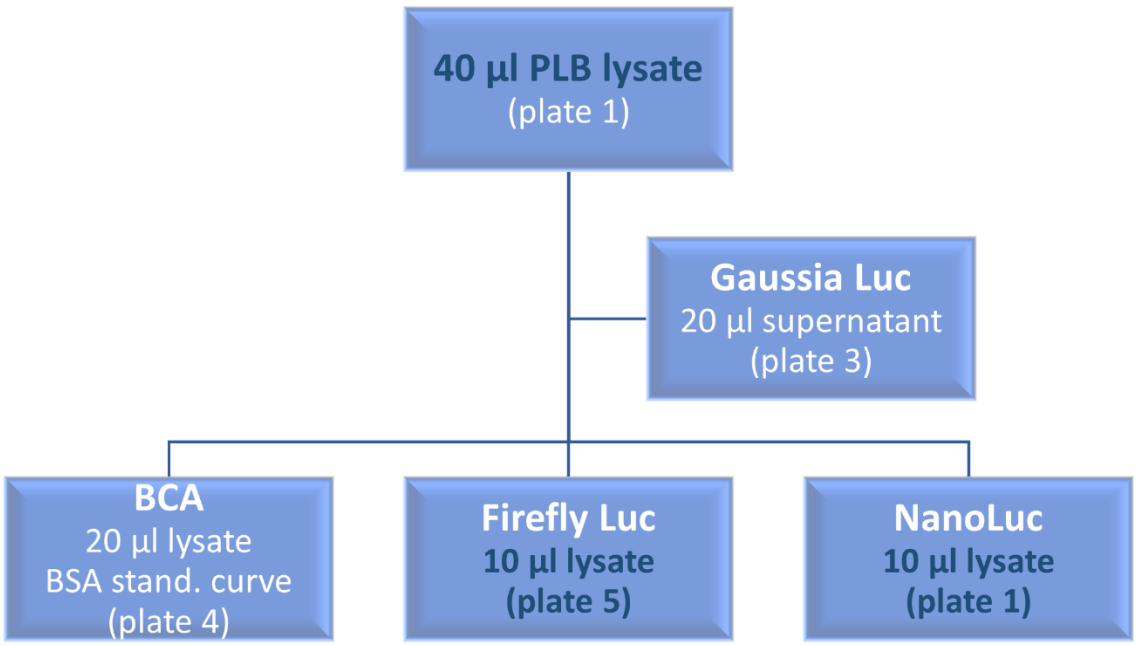

Figure 17: Schematic reading for Multi-Luc/BCA assay using the common method. Associated plates and volumes are shown in the figure. The differences to the alternative method are marked in dark blue.

The supernatant of the wells was transferred into a transparent 96-well plate (plate 2, not shown in the figure) for the Gaussia Luc assay. After washing each well of plate 1 with 200 µl PBS, the PBS was removed carefully with a vacuum aspiration system and 40 µl of PLB 1x was added. Previously, PLB 1x was prepared by diluting PLB 5x from Promega with MilliQ water in a ratio of 1:5. The following step was shaking the treated plate for 30 minutes, 500 rpm at room temperature. Although the shaking time was 30

minutes, the entire lysing duration summed up to 50 minutes. In the interim, the supernatant in plate 2 was mixed with a multichannel pipette, 20 µl of each well were transferred into a white 96-well plate (plate 3) and stored at 4°C.

After lysing the cells, each well of plate 1 was carefully scratched and 20 µl of the cell lysate were transferred into a transparent 96-well plate (plate 4) for BCA assay. This plate already contained a premade BSA standard curve, which will be described in detail in later. Out of the cell lysate in plate 1 10 µl were taken and transferred into a fresh white 96-well plate (plate 5) for Firefly Luc assay. The remaining 10 µl cell lysate in plate 1 were used for the NanoLuc assay.

While plate 1, plate 3 and plate 5 were all read with a *GloMax Multimode Microplate* reader, plate 4 was read with the *Tecan Infinite M200 Pro* reader.

For measuring the Relative Light Units (RLUs) by the Firefly Luc assay, a mixture of 100 µl of housemade Luciferase assay reagent buffer + luciferin (LBL), which was previously taken out of the -80°C freezer and kept under light protection, was directly injected into each well in question by the reader.

For measuring the RLU values by the NanoLuc assay, 40 µl of a mixture of one volume of Nano-Glo® Luciferase Assay Substrate with 50 volumes of Nano-Glo® Luciferase Assay Buffer (Promega), both at room temperature and kept under light protection, were directly injected in each well by the plate reader. At least 3 minutes wait after injection were needed before measuring the luminescence. (Promega. Technical Manual. Nano-Glo® Luciferase Assay System).

For scaling the RLU intensities by the Gaussia Luc assay, a mixture of 10.16 µl Coelenterazine (stored at -80° C) and 5089.4 µl of the housemade Coelenteranzine Assay Buffer (hCAB), consisting of PBS + 5mM sodium chloride (pH 7.2), had to incubate at least 30 minutes at room temperature and under light protection. 40 µl of this dilution were directly injected into each well containing the supernatant by the reader. The normalization of the RLU values of all these assays was done by the protein quantification using the BCA assay.

Alternative Method Without Scratching

The goal of this method was to omit scratching due to several problems which accompanied this process. For the described alternative method, the Multi-Luc/BCA assay was carried out in the same way as the common method, except for few points, which are brought up as follows.

Instead of adding 40 µl PLB 1x to each well of plate 1, 50 µl PLB 1x were used for lysing the cells, while the lysing time of 50 minutes in total remained the same.

After this, the cells of each well were only gently pipetted up and down 10 times, resulting in the cell lysate. The omission of the scratching process is the crucial difference in this method compared to the common one.

Another distinction is the transfer of 10 µl cell lysate in a white 96-well plate (plate 5) for the NanoLuc assay, instead of the Firefly Luc assay. This procedure ensures an exact amount of cell lysate for the NanoLuc assay, which is the most sensitive assay.

The remaining 20 µl cell lysate in the treated plate (plate 1) are for getting the Firefly Luc assay.

Reading the three assays with the luminometer was performed exactly in the same way as in the common method described above. The whole process is shown in Figure 18.

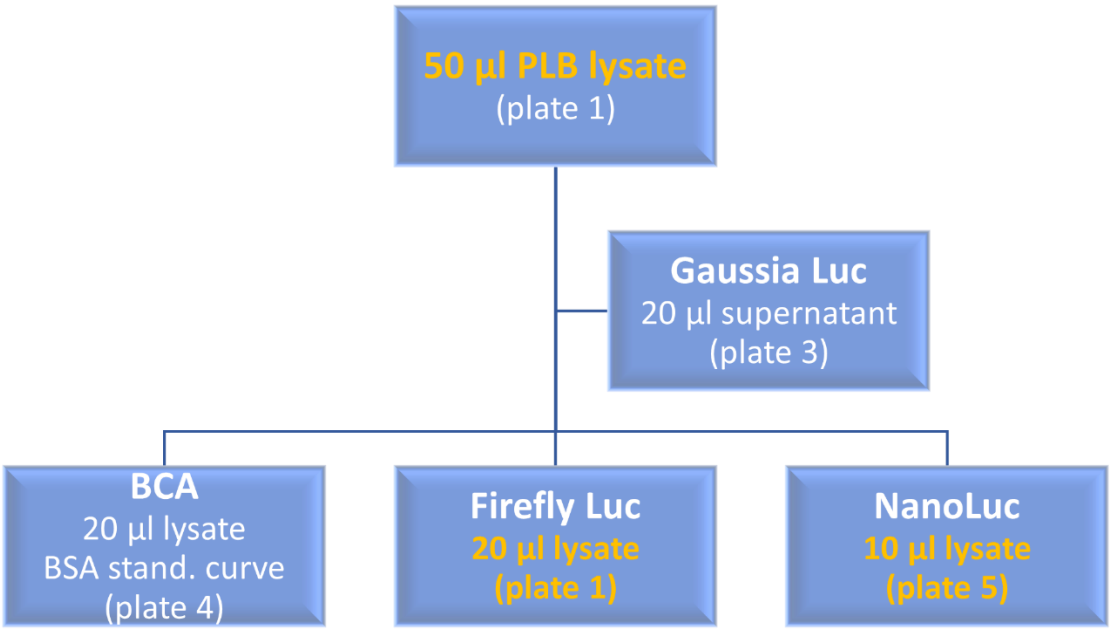

Figure 18: Schematic reading for Multi-Luc/BCA assay using the alternative method. Associated plates and volumes are shown in the figure. The differences to the common method are marked in orange.

5.2.3.2. BCA Assay

As already described, the normalization of the RLU values was based on the bicinchoninic acid assay (BCA), a highly sensitive and selective colorimetric assay for determining the protein concentration. The first step of this assay was preparing PLB 2x by mixing 300 µl of MilliQ-water with 200 µl of PLB 5x. As it can be seen in Figure 19, Bovine Serum Albumine (BSA) dilutions were made by mixing MilliQ-water, BSA 2 mg/ml and PLB 2x. 20 µl of each dilution was pipetted in triplicates into plate 4 in an ascending order, beginning with the lowest concentration (2G). The dilutions were intended to result in a standard curve.

Sample ID	MilliQ-water [µl]	BSA 2 mg/ml from Kit [µl]	**PLB 2x** [µl]	BSA µg/well
8A	-	50	50	20
7B	10	40	50	16
6C	20	30	50	12
5D	30	20	50	8
4E	40	10	50	4
3F	45	5	50	2
2G	50	-	50	-

Figure 19: Modified BSA dilution protocol (Gruber, 2021).

20 µl of PLB 1x were also added in a triplicate into plate 4, in order the substract those values as a blank from the protein amounts to get a precise determination.

200 µl of working reagent consisting of 50 parts reagent A and one part reagent B and kept under light protection, were added into each well of the plate. Subsequently, the plate was wrapped into aluminium foil due to its light sensitivity, shaken at 300 rpm for 30 seconds and kept in the incubator at 37°C for 30 minutes.

During this incubation time, a color change of the sample took place based on the reduction from Cu^{2+} to Cu^{1+} by proteins, combined with the selective colorimetric detection of Cu^{1+} by bicinchoninic acid. Both reactions together resulted in a purple-colored product, whose absorption could be measured at 562 nm with a plate reader. The intensity of the color was increasing with the protein concentration.

After cooling down the plate for 10 minutes to reach room temperature again, the plate was read by a *Tecan Infinite M200 Pro* reader using a wavelength of 562 nm, a bandwidth of 9 nm and a flash-number of 25. (Thermo Fisher)

To reach a standard curve with a coefficient of determination of at least 0.9900, preliminary trials were performed only with BSA and free of cell lysate.

By using the functional equation of the standard curve, the right protein amounts in the total cell lysate were extrapolated from the different measurement volumes (BCA: 20 µl, Firefly Luc: 10 µl/20 µl, Gaussia Luc: 20 µl, NanoLuc: 10 µl). The next calculation step was normalizing all RLU values to RLU/1 µg of protein by adapting them to the corresponding measurement volumes relative to total cell lysate amount and dividing them by the respective protein amount in the lysate. (Weiss, 2020)

5.3. Workflow for Multi-Reporter Luciferase Assay Combined with Transfection of Inducer Plasmids

For characterizing the responsiveness of the HEK293T 3P-Luc cells for pathway modulators, LPEI nanocarrier based transfections with pathway inducer plasmids were conducted. Namely, pAd (Wnt pathway inducer plasmid), phGli1 (Sonic Hedgehog pathway inducer plasmid) and phICN1 (Notch pathway inducer plasmid) were applied. As controls served a pUC19 plasmid (induces no pathway), as described in Norrander, et al., 1983, untreated cells and HBG treated cells. The activity of all three luciferases was determined for each single induction.

The principal steps for carrying out this combined assay were cell seeding into a white 96-well plate on Day 1, polyplexing as well as transfection with the inducer plasmids on Day 2 and reading the luminescence signals on Day 3 or Day 4 (24 hours respectively 48 hours after transfections), as it can be seen in Figure 20.

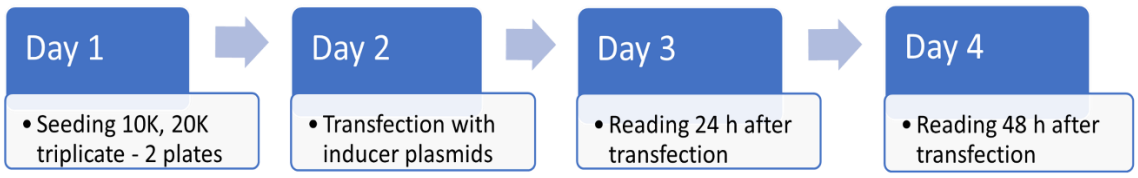

Figure 20: Workflow for the Multi-Luc assay in combination with induction.

This assay was performed with HEK293T 3P-Luc cells only by employing the alternative method without scratching, described in detail in *5.2.3.1*..

5.3.1. Cell Seeding

Seeding the cells was done as described in *5.2.2.,* except for the following modifications. Only 10,000 and 20,000 cells per well were seeded in comparison. 10,000 cells per well were seeded into the upper part of the plate, while 20,000 cells per well were seeded into the lower part. Six triplicates per cell number were seeded: One triplicate for each plasmid (pUC19, pAd, phGli, phICN1), as well as one triplicate for untreated cells and one for HBG treated cells, that both served as a control. Two completely similar plates were seeded for the read-out 24 respectively 48 hours after transfection.

5.3.2. Polyplexing and Transfection

On the second day, 24 hours after adding the polyplexes, the plate was taken out of the incubator and the medium in all wells, except for those with the untreated cells, was aspirated with the vacuum aspiration system. The next step was adding 90 µl of basal DMEM + 1000 µg/ml G418 into each well.

Previously, appropriate volumes of linear polyethyleneimine (LPEI) (10kDa) and pDNA were both diluted in HEPES buffered glucose (HBG), resulting in a N/P ratio of 9 and a final pDNA concentration of 20 µg/ml. The following equation was used for defining the appropriate amount of LPEI according to the striven N/P ratio. (Taschauer, et al., 2016):

$$m(LPEI) = \frac{m(pDNA)\ x\ molecular\ weight\ of\ one\ LPEI\ subunit\ x\ \frac{N}{P}}{average\ molecular\ weight\ of\ a\ nucleotid}$$

$$= \frac{m(pDNA)\ x\ 43\ x\ 9}{330}$$

For all four plasmids (pUC19, pAd, phGli1, phICN1) polyplexes were formed by flash-pipetting equal amounts of LPEI and pDNA dilutions, respectively. As the next step, 10 µl of polyplex solution were added into the wells dedicated to the respective treatment – except for the untreated and HBG treated ones. Thus, the total amount of plasmid

per well was 200 ng, while each well contained 100 µl volume in total. The overview of the treatment can be seen in Figure 21.

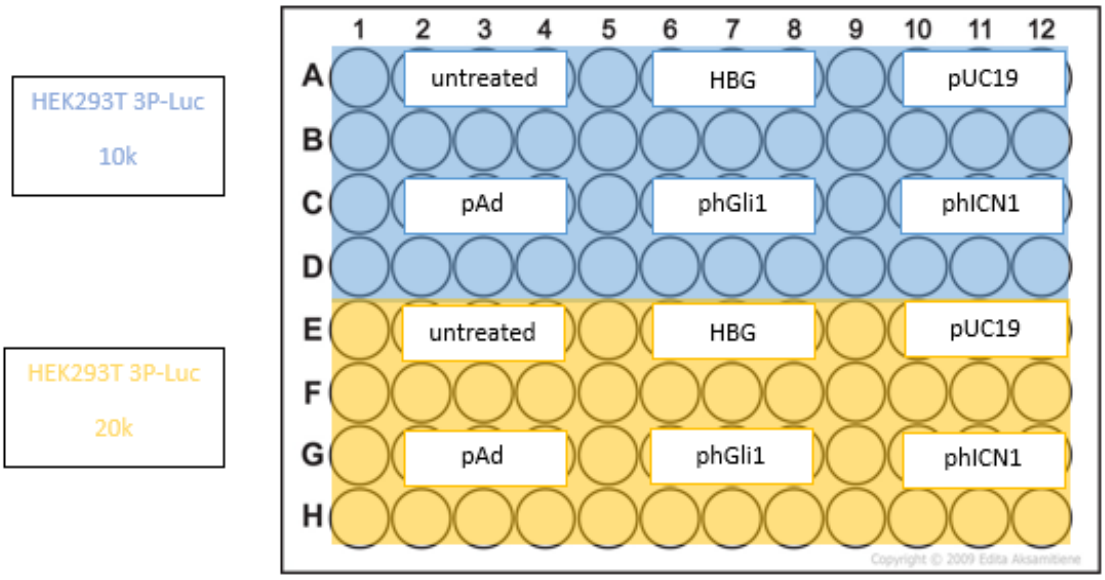

Figure 21: Schematic overview of a 96-well plate showing the different transfection treatments.

Instead of the polyplexes 10 µl HBG were added into the wells associated with the treatment with HBG only. After an incubation time of 4 hours at 37°C, another 100 µl of complete medium (DMEM + 1000 µg/ml G418) were added, resulting in 200 µl per well in summary. Afterwards, the plate incubated for another 20 hours respectively 44 hours at 37°C, depending on the treatment.

5.3.3. Reading Multi-Luc/BCA Assay

As already mentioned, the read-out of this combined assay was performed according to the investigated alternative method without scratching, as discussed in *5.2.3.1.* and whose schematic reading process was previously demonstrated in Figure 18. The Multi-Luc/BCA assay was either conducted on Day 3 (24 hours after transfections) or on Day 4 (48 hours after transfection).

5.3.4. Evaluation of EGFP Expression in HEK293T 3P-Luc Cells

As mentioned above, HEK293T 3P-Luc cells are stably transduced with the 3P-Luc plasmid harboring a CMV-driven EGFP expression cassette under constitutive expression. This results in emitting green fluorescent signals with an emission maximum of 525 nm for the purpose of detecting and sorting. In this thesis, HEK293T 3P-Luc cells were weekly characterized for EGFP expression by fluorescence microscopy using an inverted microscope from *Olympus*. This was always done after the weekend, right before splitting and seeding both cell types for new experiments. The cells were checked both using phase contrast and the FITC filter set for watching the fluorescence. The proportion of fluorescent cells was determined by comparing the density of fluorescent cells (using the FITC filter set) to the density of the whole cell layer visible under phase contrast at the same position and time. Three different locations of the flask surface were checked and compared each time, also pictures were taken for documentation. The fluorescence level was estimated after each measurement and observed in the course of time. As a control, HEK293T wt cells were also checked for EGFP expression to exclude their contamination with HEK293T 3P-Luc cells.

In addition to this weekly characterization, the EGFP-signal of both HEK293T wt and HEK293T 3P-Luc cells was determined and compared using flow cytometry finally. In this case, a *MACSQuant Analyzer 10, Miltenyi Biotec* was used and the cells were measured with the FITC channel (525/50 nm). For priming and setting the device, 100 µl of both HEK293T wt and 3P-Luc cells were injected, respectively in a 1:5 dilution with PBS. For the measurement, both HEK293T wt and 3P-Luc cells were detected in duplets in a 1:10 dilution with PBS. The data obtained from flow cytometry was analyzed using the *FlowJo* software (FlowJo™ Software, 2019) and therefore, the proportion of EGFP-positive cells in all HEK293T 3P-Luc cells could be determined. The applied gating strategy is described in detail in *6.1.3*..

5.4. Data Analysis

Due to various reasons, several conducted experiments resulted in some negative values – those are not plotted in the graphs given, only positive values are shown. This explains the lack of single categories on the X-axis in few graphs, for instance in Figure 25. All scales plotted are selected for pointing out the results and in particular demonstrating the statistical significance as clearly as possible, if necessary, even at the expense of the uniformity of all scales in one overview. The vertical standard deviations plotted are solely in the range of plus.

5.5. Statistics

In order to check the statistical significance of the gained results of the multi-reporter luciferase assay also in combination with the transfection with inducer plasmids, the Mann-Whitney U Test Calculator by *Social Science Statistics* (Statistics, 2020) was employed. A legend for the symbols describing the different levels of significance used in further graphs is displayed in Figure 22.

Mann-Whitney U Test Calculation		
Two-tailed	0.05	*
Two-tailed	0.01	**
Two-tailed	0.001	***

Figure 22: Legend for different levels of significance.

6. Results and Discussion

Characterization of Geneticin-Enriched HEK293T 3P-Luc Cells via Multi-Luc/BCA Assay

6.1. Simultaneous Detection of Multiple Pathway Activity

As mentioned previously, one major goal of this project was to study geneticin-enriched lentivirally stably transduced HEK293T 3P-Luc cells for the activity of the Sonic Hedgehog, Notch and Wnt pathway. The concept of multiplexing was employed by reading out the Firefly Luc assay for determining the Hedgehog pathway activity, the Gaussia Luc assay for characterizing the Notch pathway activity and the NanoLuc assay for evaluating the Wnt pathway activity. In addition, the fourth assay in this multiplexing sequence was the BCA assay for normalization of the RLU values according to the respective protein amount. The activity of the signaling pathways correlates with the measured and normalized RLU values within the respective luciferase assay.

As already mentioned, the scratching part of the common method of the Multi-Luc/BCA assay causes various issues. For example, a high amount of cell lysate is lost during the process of scratching. This leads to an insufficient amount of cell lysate available for further assays. Due to these limitations, an alternative method for reading this multiplex assay without the scratching process was investigated in the course of this work. For a direct comparison, all conducted Multi-Luc/BCA assays on HEK293T 3P-Luc cells were performed using both methods and the gained results were compared and interpreted. The workflow and procedure of those methods differ slightly, which was explained in detail above. In all experiments, HEK293T wt cells served as a control to estimate the background signals and gain clear assignment of the detected activity of the geneticin-enriched HEK293T 3P-Luc cells. All assays were conducted in triplicates in different cell seeding densities (10,000, 20,000, 40,000 and 80,000 cells per well) after an incubation time of 24 hours and 48 hours in order to determine the most appropriate cell number and duration regarding the signal intensity and consistency. For ensuring

the reproducibility of the results, each assay was repeated three times at least, the demonstrated results are averaged to the three most representative runs.

At first, a BCA standard curve providing a coefficient of determination (R^2) of at least 0.9900 was created each time for enabling protein amount normalization. A representative standard curve is demonstrated in Figure 23.

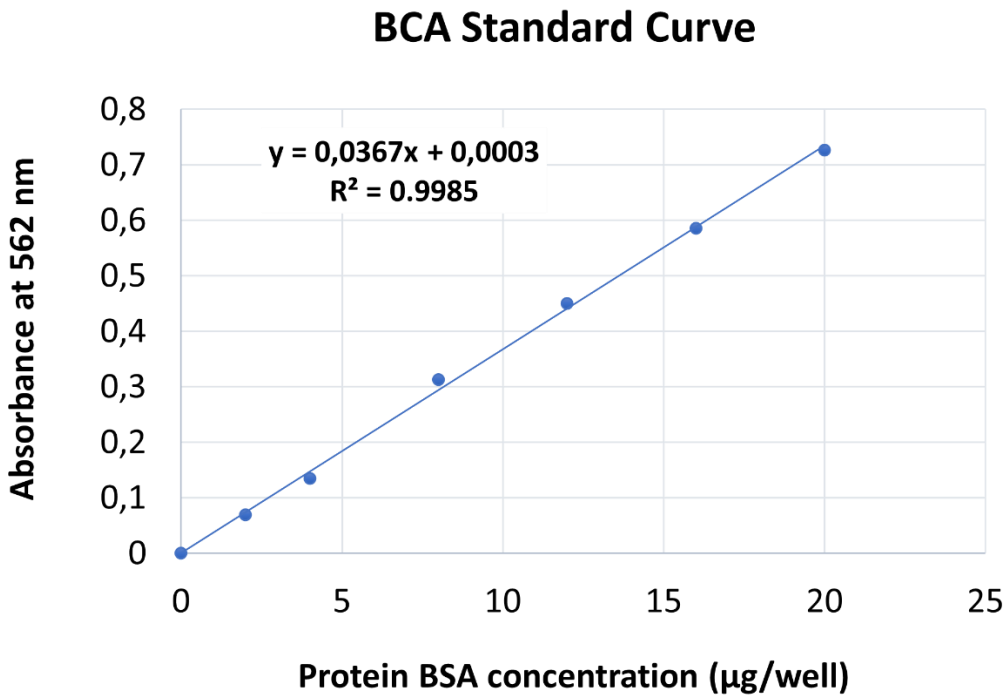

Figure 23: Representative standard curve utilized for protein amount normalization using a *Tecan Infinite M200 Pro* reader at 562 nm wavelength.

Figure 24 describes the protein amount of both HEK293T wt and 3P-Luc cells for 24 hours and 48 hours after seeding employing the BCA assay. The common method was compared with the alternative method without scratching. The variance of the increasing bars of each single experiment can be described with the coefficient of determination (R^2). Here only the R^2 values of HEK293T 3P-Luc cells are shown.

For scratching, as shown in Figure 24A and 24B, both HEK293T wt and 3P-Luc cells show different patterns. While 24 hours after seeding (Fig. 24A), the protein amounts are very

low, the graph shows higher protein amounts after an incubation time of 48 hours (Fig. 24B). The increase of HEK293T 3P-Luc cell signals determined by R^2 is more proportional after 24 hours (R^2 = 0.9393) compared to the one after 48 hours (R^2 = 0.9052). In the experiment without scratching (Fig. 24C and 24D), both HEK293T wt and 3P-Luc cells were tested as well. 24 hours after seeding (Fig. 24C), low protein amounts are detected, especially for 10,000 and 20,000 cells. 48 hours after seeding (Fig. 24D) the protein amounts are much higher and the different amounts of wt and 3P-Luc cells are more similar. In this run, the increase of the protein amounts of HEK293T 3P-Luc cells (R^2 = 0.9911) is considerably more proportional than after 24 hours without scratching (R^2 = 0.9349).

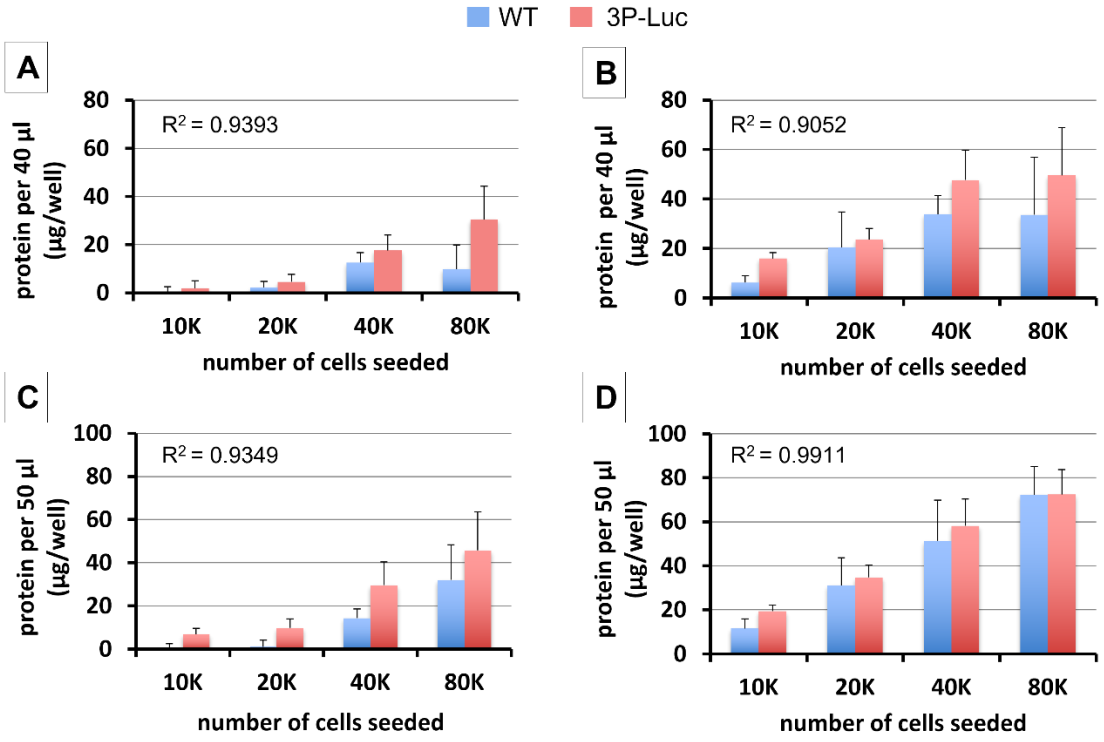

Figure 24: Protein amount of HEK293T 3P-Luc cells (as compared to HEK293T wt cells) via BCA assay. Different numbers of cells per well were seeded and Multi-Luc/BCA assay was performed by using the method with scratching i.e. protein per 40 µl (µg/well) (A and B) or without scratching i.e. 50 µl (µg/well) (C and D). Protein amount data after 24h (A and C) or 48h (B and D) is plotted as average from three independent experiments. R^2 values are for HEK293T 3P-Luc cells. n = xy + stddev.

Although the BCA assay itself worked fine, the protein estimations are not precise and proportional to the number of cells seeded for most of the experiments. The protein amounts after 24 hours of incubation are very low. Nevertheless, after both durations the method without scratching shows higher protein amounts in total, compared to the method with scratching. The method without scratching 48 hours after seeding provides the highest coefficient of determination ($R^2 = 0.9911$) for HEK293T 3P-Luc cells. The method without scratching reveals higher coefficients of determination in total and therefore a higher proportionality of the increasing protein amounts according to the cell number. This indicates a higher accuracy than the method with scratching. The potential overspill and complete loss of cell lysate while scratching might be one explanation for this.

Protein amounts from different treatments are needed for normalization of luciferase expression data from the different luciferase assays. However, if protein estimation is imprecise the normalization of luciferase data is not correct and will not be the same for different treatments. This is visible in Figure 25 where Firefly luciferase read-out was normalized by protein from BCA assay and it can be observed that normalization does not work uniformly for all cell seeding numbers and different treatments. Also, some values were negative so only positive values were displayed.

In experiments including scratching, as shown in Figure 25A and 25B, both HEK293T wt and 3P-Luc cells were tested. After an incubation time of 24 hours (Fig. 25A), the normalized values are very inconsistent and the activity of 20,000 3P-Luc cells is even in the negative area. 48 hours after seeding (Fig. 25B), these values are also poor and two categories are in the negative area. The experiments without scratching (Fig. 25C and 25D) were also conducted with HEK293T wt and 3P-Luc cells. The results for 24 hours after seeding (Fig. 25C) are very poor and low. This also applies to the results 48 hours after seeding (Fig. 25D), where only the activities for 10,000 and 20,000 cells are detectable. In comparison, the common method with scratching reveals slightly better results, however the values are poor and not usable.

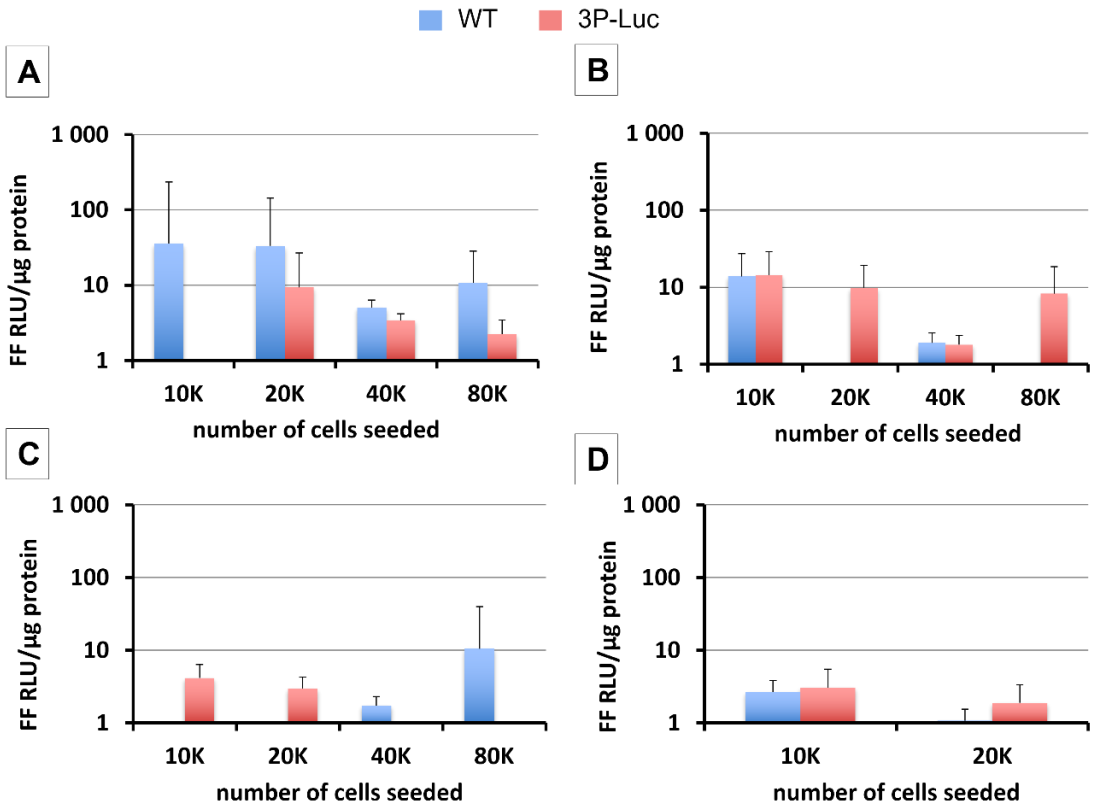

Figure 25: Normalized Hedgehog pathway activity estimation in HEK293T 3P-Luc cells (as compared to HEK293T wt cells) via Firefly luciferase read-out from Multi-Luc/BCA assay. Different numbers of cells per well were seeded and the Multi-Luc/BCA assay was performed by using the method with scratching (A and B) or without scratching (C and D). Firefly luciferase expression data normalized by protein i.e. RLU/µg protein after 24h (A and C) or 48h (B and D) is plotted as average from three independent experiments. n = xy + stddev.

It is striking that all the results – regardless of the method or the incubation time – are inconsistent and inappropriate for further interpretations, traceable to the poor raw protein amounts, as shown in Figure 24.

Figure 25 is just a representative graph plotted to show that BCA normalized luciferase data might be error prone. (The respective normalized data of both the Notch and Wnt pathway read-out is displayed in the appendix). Thus, for all subsequent experiments, non-normalized luciferase data is plotted i.e. RLU values per whole lysate, not normalized by the respective protein amount.

Figure 26 shows Firefly luciferase signals, indicating the Hedgehog pathway activity, in its non-normalized version, reporting the raw RLU values. The displayed RLU values are originated from 40 µl cell lysate in the method including scratching or from 50 µl cell lysate in the method without scratching.

Figure 26A and 26B describe the experiments with scratching with both HEK293T wt and 3P-Luc cells. 24 hours after seeding (Fig. 26A), the values of 3P-Luc cells do not differ from those of wt cells, indicating no specific pathway activity. For 48 hours after seeding (Fig. 26B), the activities of 3P-Luc and wt cells are slightly different, especially with 80,000 cells seeded. In the experiments without scratching (Fig. 26C and 26D) after an incubation time of 24 hours (Fig. 26C) and 48 hours (Fig. 26D), the values for 3P-Luc cells are not significantly higher than those for wt cells.

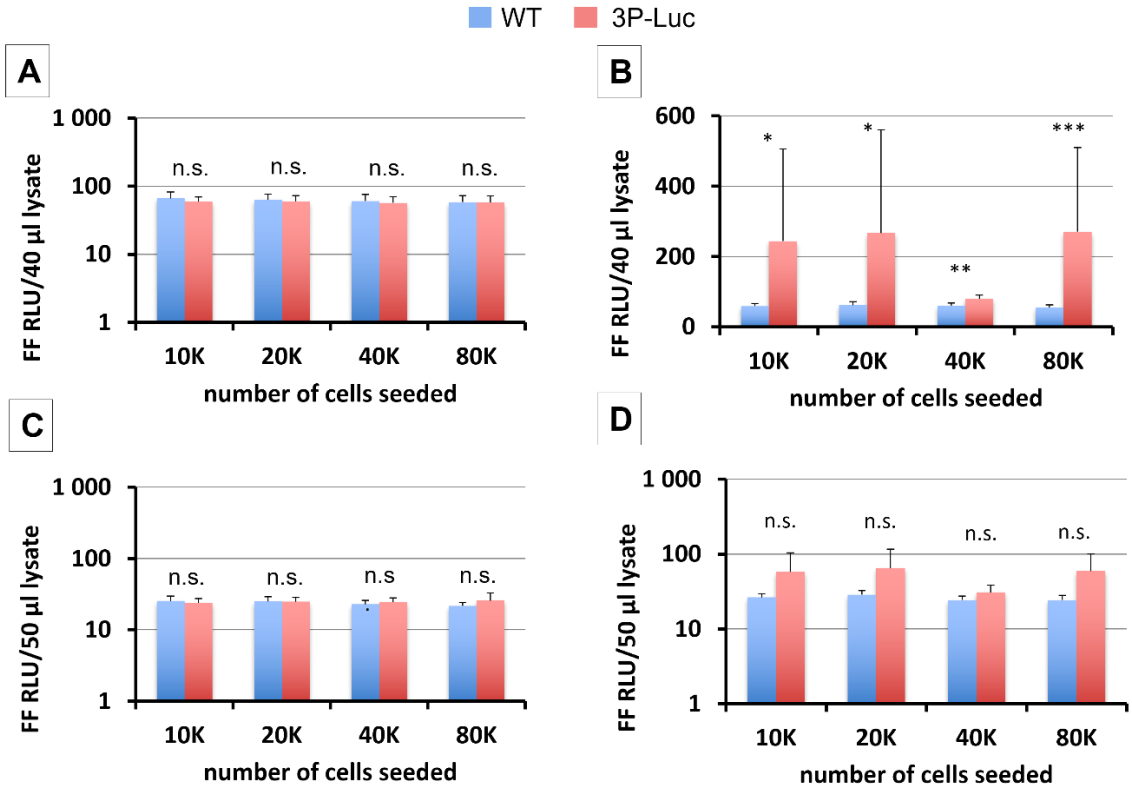

Figure 26: Hedgehog pathway activity estimation in HEK293T 3P-Luc cells (as compared to HEK293T wt cells) via Firefly luciferase read-out from Multi-Luc/BCA assay. Different numbers of cells per well were seeded and the Multi-Luc/BCA assay was performed by using the method with scratching i.e. 40 µl lysate (A and B) or without scratching i.e. 50 µl lysate (C and D). Non-normalized Firefly luciferase expression data after 24h (A and C) or 48h (B and D) is plotted as average from three independent experiments (each with three replicates; *P< .05, **P< .01, ***P< .001, n.s.= not significant; Mann-Whitney U Test.). n = xy + stddev.

Across both methods and incubation durations, the Firefly luciferase signal is not significantly detectable, except for the method including scratching 48 hours after seeding, where the respective differences between the RLU values of the 3P-Luc and wt cells are statistically significant, yet in context only slightly detectable.

Figure 27 displays the Gaussia luciferase read-out, stating the Notch pathway activity in its non-normalized version, demonstrating the raw RLU values. The displayed RLU values are all from 200 µl supernatant.

For scratching, as shown in Figure 27A and 27B, the activity of both HEK293T wt and 3P-Luc cells was determined. 24 hours (Fig. 27A) after seeding, the values are very strong,

highly significant and provide a proportional increase according to the cell count. This also applies for the experiment after 48 hours of incubation time (Fig. 27B), where the values are even one logarithmic unit higher. For the experiments without scratching (Fig. 27C and 27D), also HEK293T 3P-Luc and wt cells were compared. The results of both methods used are almost identical.

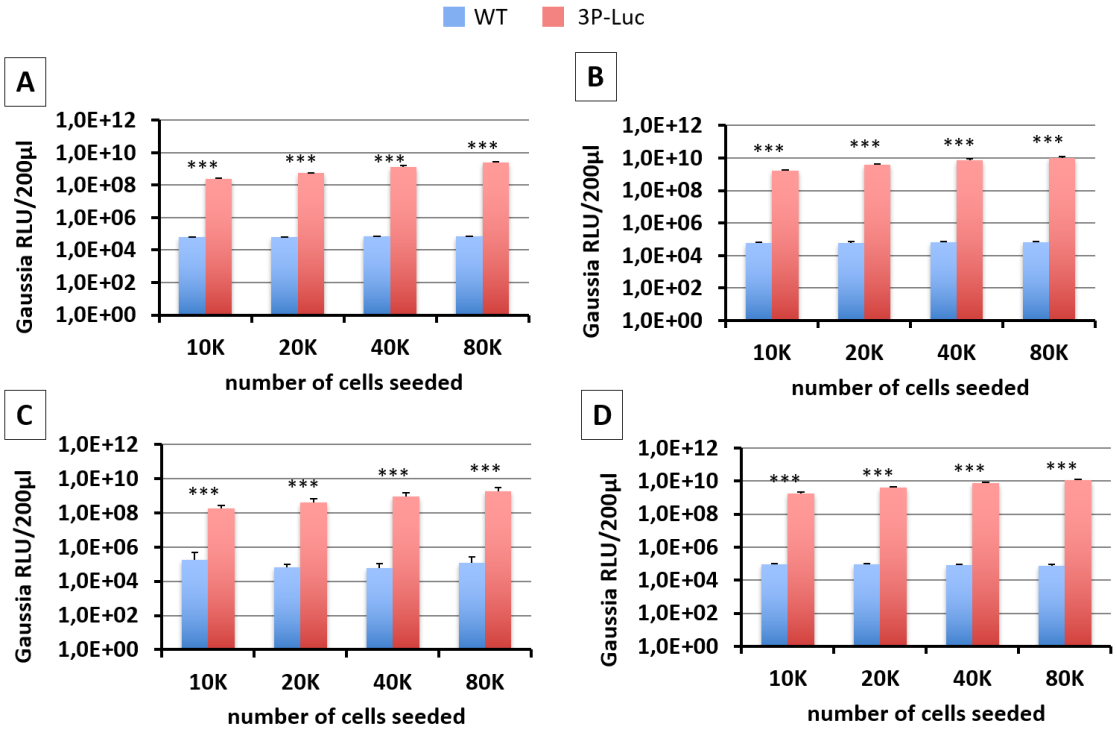

Figure 27: Notch pathway activity estimation in HEK293T 3P-Luc cells (as compared to HEK293T wt cells) via Gaussia luciferase read-out from Multi-Luc/BCA assay. Different numbers of cells per well were seeded and the Multi-Luc/BCA assay was performed by using the method with scratching (A and B) or without scratching (C and D), all plotted as Gaussia RLU/200 µl. Non-normalized Gaussia luciferase expression data after 24h (A and C) or 48h (B and D) is plotted as average from three independent experiments (each with three replicates; *P< .05, **P< .01, ***P< .001, n.s.= not significant; Mann-Whitney U Test.). n = xy + stddev.

In contrast to the Hedgehog pathway activity, the Notch pathway activity is not only very strong but also highly significantly detectable and increases proportionally to the cell count, regardless of the utilized technique or incubation time. The values of the experiments carried out after 48 hours of incubation are around one logarithmic unit higher than those 24 hours after seeding, explained by the higher cell density due to

their longer growing time. As expected, differences between the results of the two lysis methods are not detectable since it is the supernatant that is used for the Gaussia Luc assay, compared to the Firefly Luc and NanoLuc assay, whose performance requires the cell lysate. The supernatant, in contrast, is taken for analysis way before the cell lysing process takes place and is consequently not affected by the presence or absence of scratching.

Figure 28 demonstrates the non-normalized NanoLuc read-out, linked with the Wnt pathway activity. The displayed raw RLU values are from 40 µl cell lysate in the common method including scratching or from 50 µl cell lysate using the alternative method without scratching.

In experiments including scratching, as shown in Figure 28A and 28B, both HEK293T wt and 3P-Luc cells were tested. After an incubation time of 24 hours (Fig. 28A), the values are low, show no proportional rise according to the cell number and the pathway activity is not significantly detectable. 48 hours after seeding (Fig. 28B), the NanoLuc signal is also not increasing proportionally to the cell count, but the pathway activity is significantly detectable. Here, only the activity of 40,000 cells seeded is highly significant. For experiments without scratching, (Fig. 28C and 28D), also both cell types were used for comparison. 24 hours after seeding (Fig. 28C), the values are weak, but the pathway activity is significantly detectable in all cell numbers except for 10,000. The values are becoming more significantly detectable with the ascending cell count. The pathway activity of 40,000 and 80,000 cells is even highly significantly detectable. After 48 hours of incubation time (Fig. 28D), the signals are very strong, show a proportional rise to their cell number and are all detectable with high statistical significance. Therefore, this combination of method and duration provides the best results.

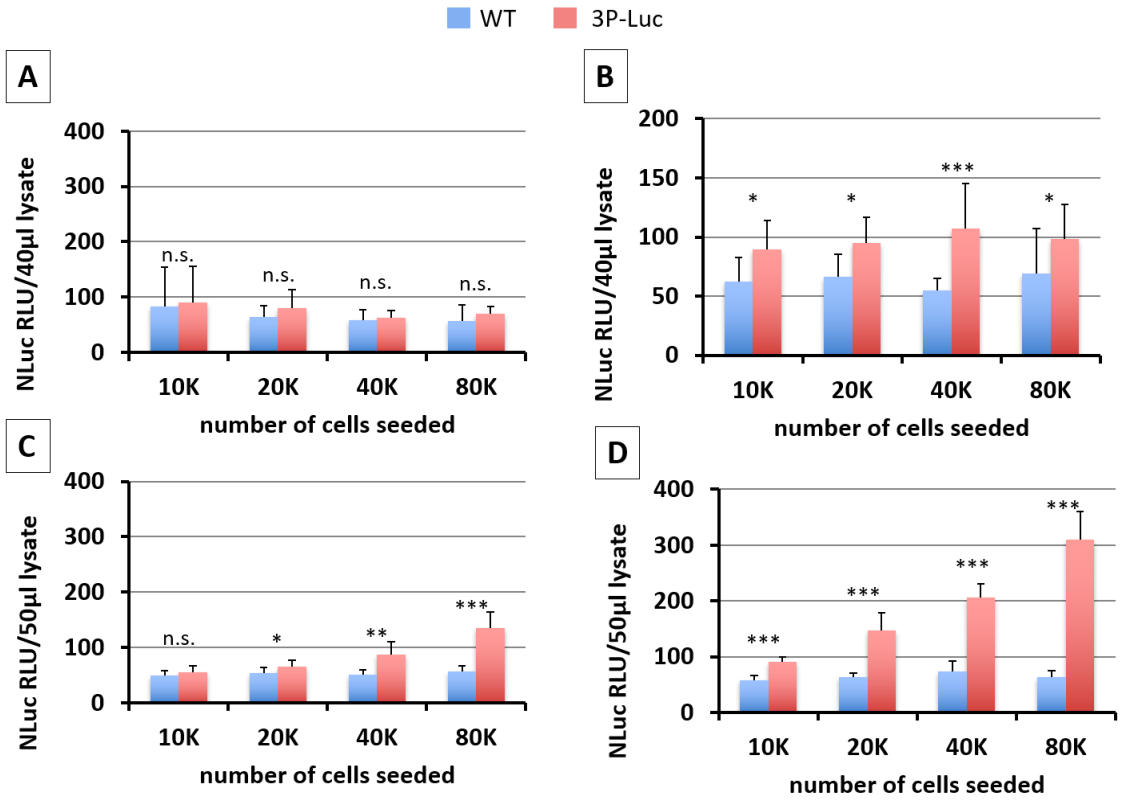

Figure 28: Wnt pathway activity estimation in HEK293T 3P-Luc cells (as compared to HEK293T wt cells) via NanoLuc read-out from Multi-Luc/BCA assay. Different numbers of cells per well were seeded and the Multi-Luc/BCA assay was performed by using the method with scratching i.e. 40 µl lysate (A and B) or without scratching i.e. 50 µl lysate (C and D). Non-normalized NanoLuc expression data after 24h (A and C) or 48h (B and D) is plotted as average from three independent experiments (each with three replicates; *P< .05, **P< .01, ***P< .001, n.s.= not significant; Mann-Whitney U Test.). n = xy + stddev.

The signals after 48 hours incubation time of both methods gave a higher statistical significance than those of the experiments 24 hours after seeding. Probably this can be traced to the longer growing time leading to a higher cell density. In all, the NanoLuc signal increases more proportionally to the cell number and is markedly higher significant by using the alternative method without scratching. A possible reason for the irregular results and the absence of a rise proportional to the cell number in the technique using scratching may be the scratching part itself. According to the challenges accompanying scratching, which were mentioned previously, a potential overspill while scratching owing to their physical proximity might have happened. Physical separation of the wells in question could pose a potential solution for this problem but also

requires more well plates, which come along with higher costs. Moreover, also a partly loss of the cell lysate by splattering during scratching is evident. Both issues may be possible explanations for such results, very likely a combination of them.

When comparing these results with the findings of Silvia Weiss (Weiss, 2020; who previously performed this Multi-Luc/BCA assay on HEK293T wt cells but with transient transfections with the 3P-Luc plasmid) it can be stated that few results are similar and some are different. While in both theses, Sonic Hedgehog pathway is found to show the lowest activity of all three pathways, its activity was – in contrast to the present findings – significantly detectable in Weiss 2020. Another disparity is the Wnt pathway activity, which was measurable for both durations in transiently transfected HEK293T cells, while here only significantly detectable for 48 hours incubation time. The measured intensities of the Notch pathways, though, are very close to those of Weiss, 2020. A possible explanation for these distinct results might be minimal disparities in the applied method. Another possible reason might include an unexpected functionality of the HEK293T 3P-Luc cells compared to the transient transfected HEK293T cells with this multi-reporter plasmid, regarding the expression of the Firefly luciferase. For gaining closer comparison, further research with sorted HEK293T 3P-Luc cells is definitely required.

6.2. Pathway Induction Mediated Detection of Multiple Pathway Activity

This subsection is dedicated to the second aim of the thesis: Investigating pathway induction by inducer plasmids in HEK293T 3P-Luc cells in all three stated pathways, which were enriched with 1000 µg/ml Geneticin to characterize the responsiveness of these cells for pathway modulators. Therefore, different pathway-inducer plasmids were employed. 200 ng per well of the respective inducer plasmid were used. As control and reference pUC19 was selected, since it induces no pathway. Additional controls provided both untreated HEK293T 3P-Luc cells and HEK293T 3P-Luc cells only treated with HBG, the buffer used. All assays were carried out in triplicates in two different cell seeding densities (10,000 and 20,000 cells per well) after 24 hours and 48 hours of transfection with the respective inducer plasmid to determine the most appropriate cell number and duration regarding the signal intensity and consistency. For ensuring the reproducibility of the results, each assay was repeated three times at least. The demonstrated results were averaged to the three most representative runs. Owing to the better and more significant results gained by the alternative method without scratching in the experiment row with Multi-Luc/BCA assays alone, as it can be seen above, the experiments in this section were conducted by solely using the technique without scratching. The presence or absence of the inducibility of the three signaling pathways by respective inducer plasmids is assessed by comparing the values of cells treated with the respective inducer plasmid with the activity intensity of pUC19 treated cells.

Figure 29 illustrates the protein amount measured for HEK293T 3P-Luc cells after the transfection with the inducer plasmids by employing the Multi-Luc/BCA assay. Values of untreated cells (UT), cells treated with HBG only (corresponding to the same volume of polyplexes added per well and serving as buffer control) and plasmid-based polyplex treated cells are shown. As such, the cells were either treated with the corresponding inducer plasmid or with the pUC19 plasmid that served as transfection control.

The protein amounts of 10,000 cells seeded (Fig. 29A and 29B) 24 hours after transfection (Fig. 29A) are very low and therefore not usable. In contrast, the protein amounts 48 hours after transfection (Fig. 29B) are higher and more convincing. Graph C and D display the results of 20,000 cells seeded. Both the protein amounts of 24 hours (Fig. 29C) and 48 hours after transfection (Fig. 29D) are usable, but the experiment after 48 hours delivers higher amounts.

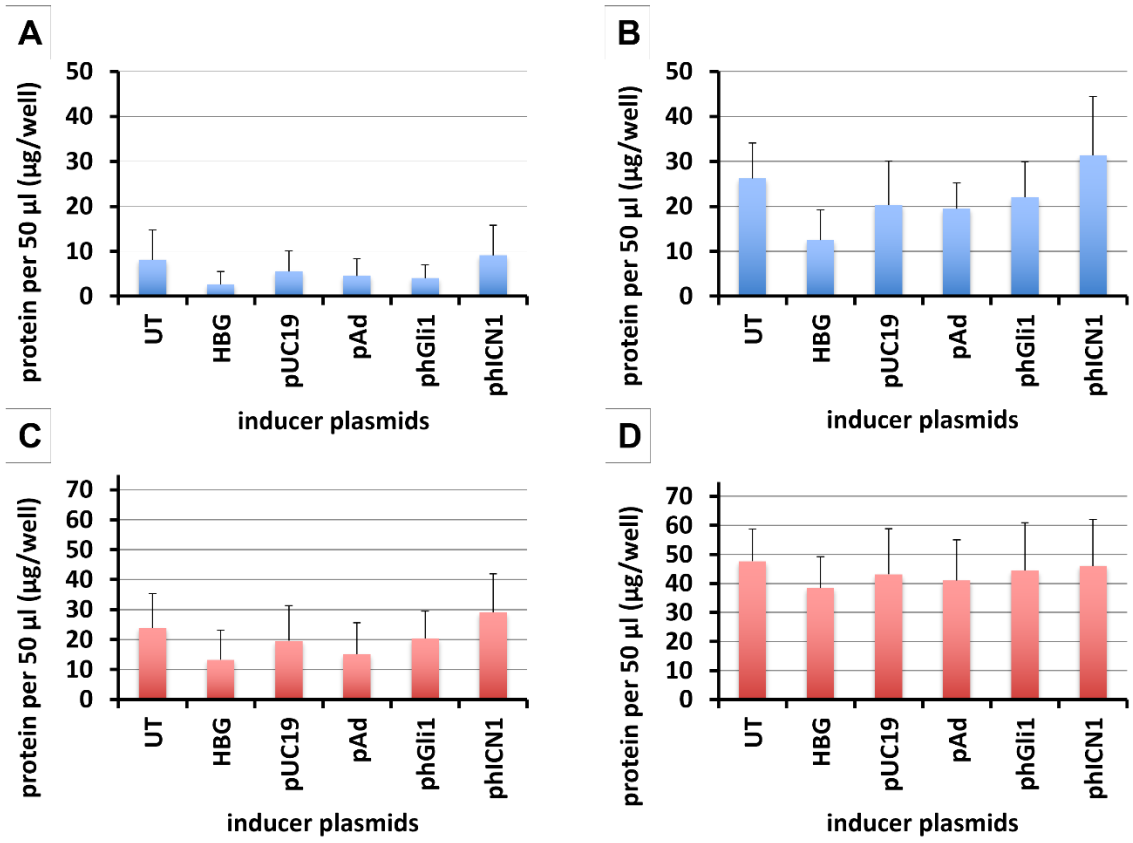

Figure 29: Protein amount of HEK293T 3P-Luc cells after transfection with pathway-inducer plasmids via Multi-Luc/BCA using the alternative method without scratching. Different cell densities were seeded for a day and then treated with different plasmid based polyplexes (pUC19-control plasmid; pAd-Wnt pathway inducer; phGli1-Hedgehog pathway inducer; phICN1-Notch pathway inducer) or HBG buffer or were left untreated (UT). BCA assay was performed with 10,000 cells per well (A and B) or 20,000 cells per well (C and D); 24h (A and C) or 48h (B and D) after transfection with pathway-inducer plasmid based polyplexes. Protein amount is plotted as protein amount per 50 µl (µg/well).
Plotted data is averaged from three independent experiments. n = xy + stddev.

As observed in earlier experiments, the protein amount differs. In general, the results of the assays 48 hours after transfection are way higher than those of 24 hours after transfection, owing to the higher cell density after a longer incubation time. Due to their lowliness, the results of 10,000 seeded cells 24 hours after transfection are not appropriate for further use. A possible reason for such poor values might be the used lysis technique without scratching.

In the following graphs, the yellow bars indicate the activity of the cells treated with the respective inducer plasmid, which is supposed to increase the RLU values of the corresponding pathway in case of a successful pathway induction.

Figures 30 demonstrates Hedgehog pathway read-out by the phGli1 inducer plasmid in HEK293T 3P-Luc cells in its non-normalized and normalized (by the corresponding protein amount) version for 10,000 cells seeded. Both the non-normalized graphs (Fig. 30A and 30B), as well as the normalized graphs (Fig. 30C and 30D) show no significant pathway induction, neither 24 hours (Fig. 30A and 30C) nor 48 hours after transfection (Fig. 30B and Fig. 30D).

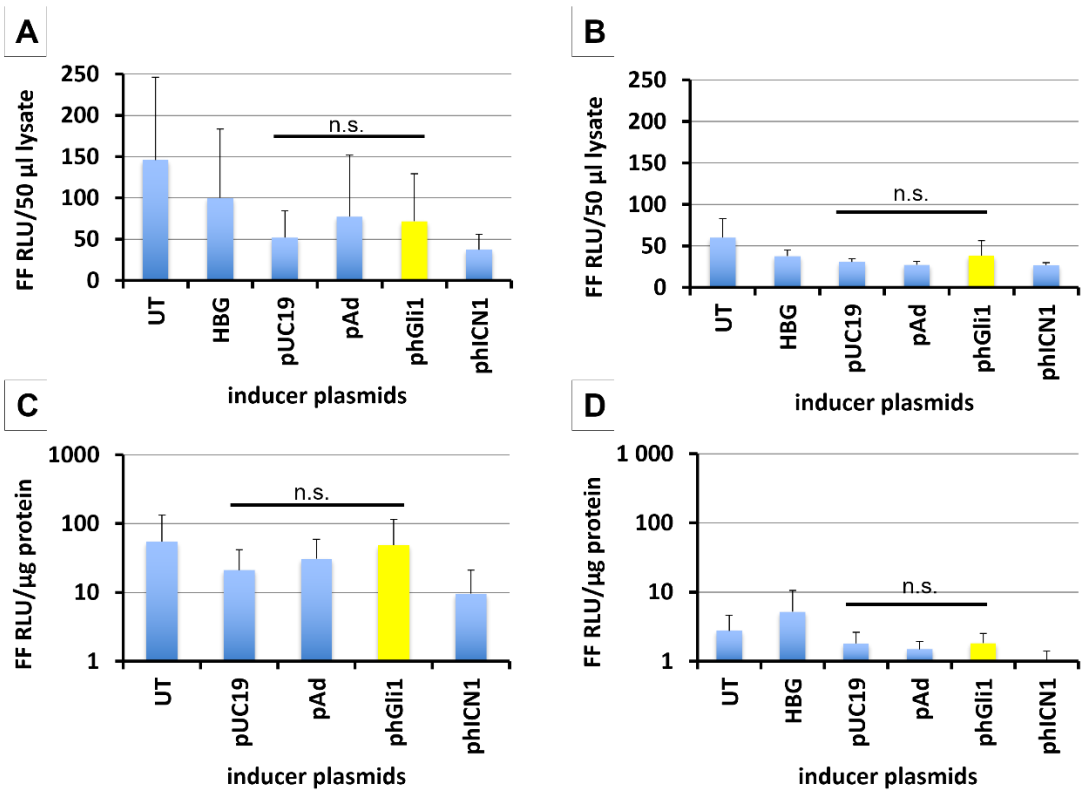

Figure 30: Hedgehog pathway activity estimation in HEK293T 3P-Luc cells (via Firefly luciferase read-out from Multi-Luc/BCA assay) after transfection with pathway-inducer plasmids. 10,000 cells were seeded for a day and then treated with different plasmid based polyplexes (pUC19-control plasmid; pAd-Wnt pathway inducer; phGli1-Hedgehog pathway inducer; phICN1-Notch pathway inducer) or HBG buffer or were left untreated (UT). Multi-Luc/BCA assay was performed by using the method without scratching 24h (A and C) or 48h (B and D) after transfection. Firefly luciferase expression is plotted as non-normalized i.e. FF RLU/50 µl lysate (A and B) and normalized by protein amount i.e. FF RLU/µg protein (C and D). The yellow bar marks the activity of the inducer plasmid relevant for Hedgehog pathway. Plotted data is averaged from three independent experiments (each with three replicates; *P< .05, **P< .01, ***P< .001, n.s.= not significant; Mann-Whitney U Test.). n = xy + stddev.

Figures 31 describes the induction of the Hedgehog pathway by the phGli1 inducer plasmid in HEK293T 3P-Luc cells in its non-normalized and normalized (by the corresponding protein amount) version for 20,000 cells seeded. Both the non-normalized graphs (Fig. 31A and 31B), as well as the normalized graphs (Fig. 31C and 31D) show no significant pathway induction, neither 24 hours (Fig. 31A and 31C) nor 48 hours after transfection (Fig. 31B and 31D). The normalized values 48 hours after transfection are even in the negative area and therefore not properly assessable.

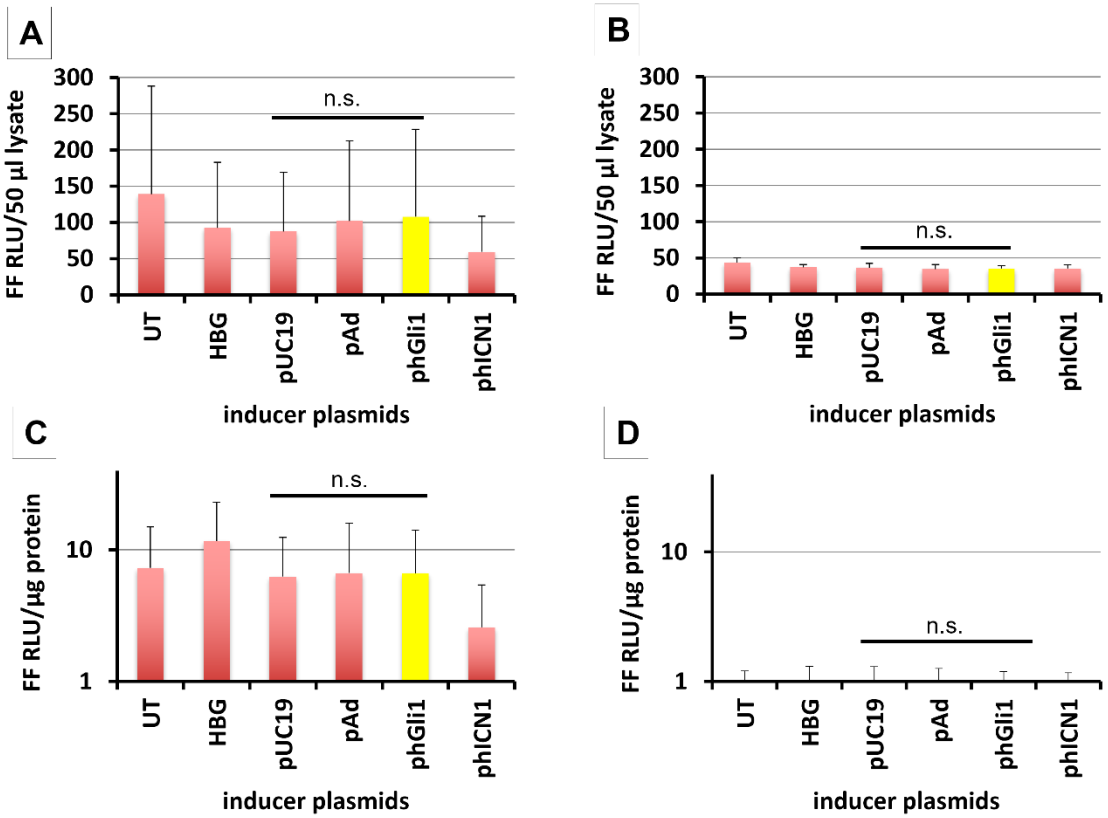

Figure 31: Hedgehog pathway activity estimation in HEK293T 3P-Luc cells (via Firefly luciferase read-out from Multi-Luc/BCA assay) after transfection with pathway-inducer plasmids. 20,000 cells were seeded for a day and then treated with different plasmid based polyplexes (pUC19-control plasmid; pAd-Wnt pathway inducer; phGli1-Hedgehog pathway inducer; phICN1-Notch pathway inducer) or HBG buffer or were left untreated (UT). Multi-Luc/BCA assay was performed by using the method without scratching 24h (A and C) or 48h (B and D) after transfection. Firefly luciferase expression is plotted as non-normalized i.e. FF RLU/50 µl lysate (A and B) and normalized by protein amount i.e. FF RLU/µg protein (C and D). The yellow bar marks the activity of the inducer plasmid relevant for Hedgehog pathway. Plotted data is averaged from three independent experiments (each with three replicates; *P< .05, **P< .01, ***P< .001, n.s.= not significant; Mann-Whitney U Test.). n = xy + stddev.

Figures 32 shows the induction of the Notch pathway by the phICN1 inducer plasmid in HEK293T 3P-Luc cells in its non-normalized and normalized (by the corresponding protein amount) version for 10,000 cells seeded. Both the non-normalized graphs (Fig. 32A and 32B), as well as the normalized graphs (Fig. 32C and 32D) show no significant pathway induction, neither 24 hours (Fig. 32A and 32C) nor 48 hours after transfection (Fig. 32B and 32D).

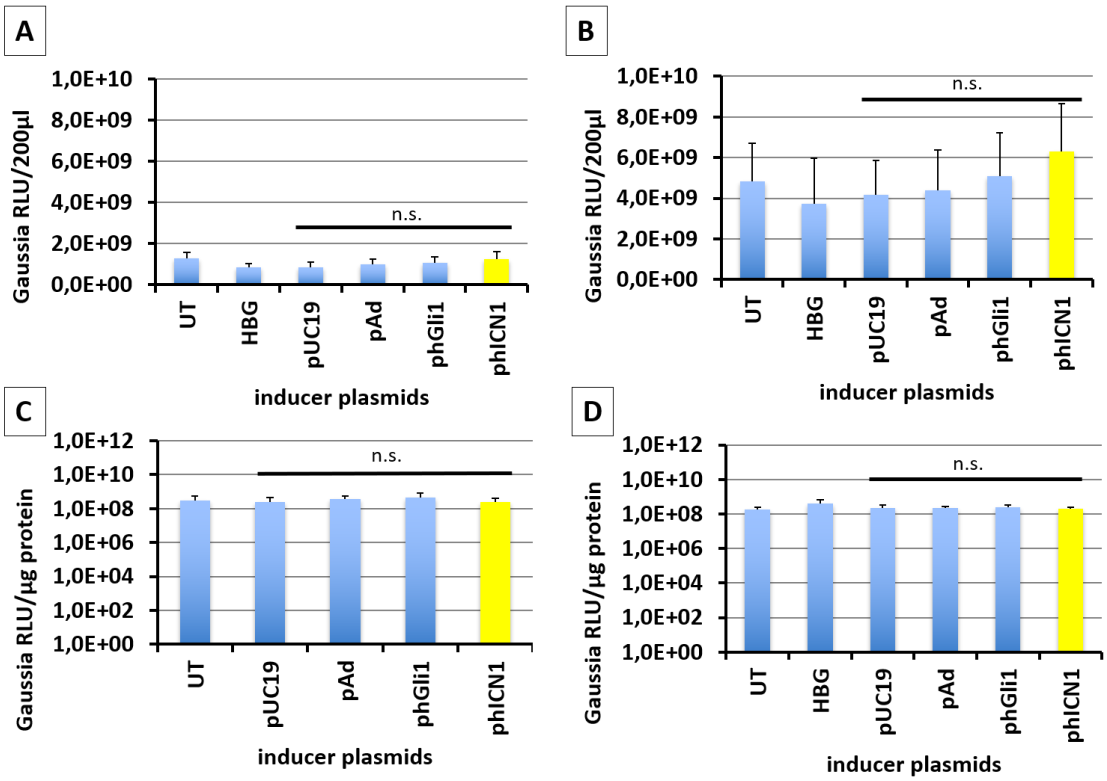

Figure 32: Notch pathway activity estimation in HEK293T 3P-Luc cells (via Gaussia luciferase read-out from Multi-Luc/BCA assay) after transfection with pathway-inducer plasmids. 10,000 cells were seeded for a day and then treated with different plasmid based polyplexes (pUC19-control plasmid; pAd-Wnt pathway inducer; phGli1-Hedgehog pathway inducer; phICN1-Notch pathway inducer) or HBG buffer or were left untreated (UT). Multi-Luc/BCA assay was performed by using the method without scratching 24h (A and C) or 48h (B and D) after transfection. Gaussia luciferase expression is plotted as non-normalized i.e. Gaussia RLU/200 µl (A and B) and normalized by protein amount i.e. Gaussia RLU/µg protein (C and D). The yellow bar marks the activity of the inducer plasmid relevant for Notch pathway. Plotted data is averaged from three independent experiments (each with three replicates; *P< .05, **P< .01, ***P< .001, n.s.= not significant; Mann-Whitney U Test.). n = xy + stddev.

Figures 33 displays the induction of the Notch pathway by the phICN1 inducer plasmid in HEK293T 3P-Luc cells in its non-normalized and normalized (by the corresponding protein amount) version for 20,000 cells seeded. Both the non-normalized Notch read-outs after 24 hours (Fig. 33A) and 48 hours (Fig. 33B), as well as the normalized read-out after 48 hours (Fig. 33D) show no significant pathway induction. In the graph displaying the normalized values of the experiment after 24 hours (Fig. 33C), even the cells treated with the control plasmid pUC19 give a significantly higher signal than the cells treated with phICN1, the inducer plasmid.

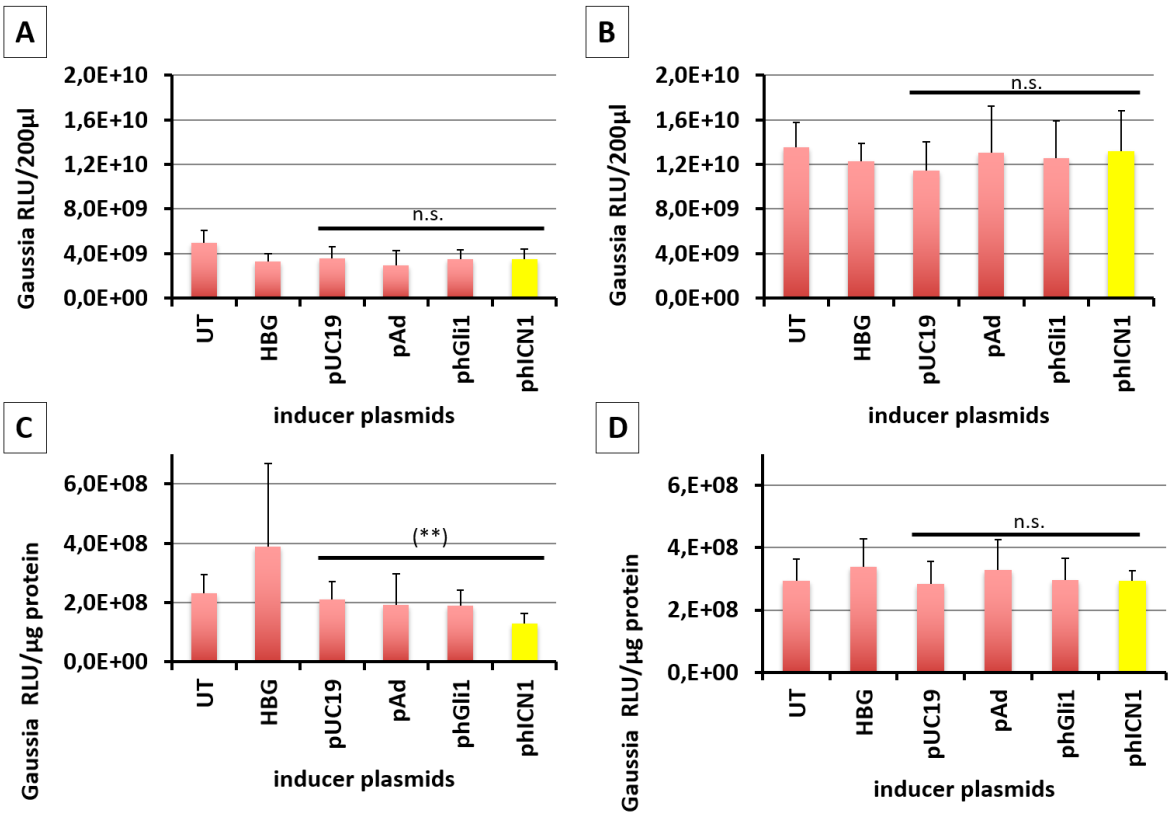

Figure 33: Notch pathway activity estimation in HEK293T 3P-Luc cells (via Gaussia luciferase read-out from Multi-Luc/BCA assay) after transfection with pathway-inducer plasmids. 20,000 cells were seeded for a day and then treated with different plasmid based polyplexes (pUC19-control plasmid; pAd-Wnt pathway inducer; phGli1-Hedgehog pathway inducer; phICN1-Notch pathway inducer) or HBG buffer or were left untreated (UT). Multi-Luc/BCA assay was performed by using the method without scratching 24h (A and C) or 48h (B and D) after transfection. Gaussia luciferase expression is plotted as non-normalized i.e. Gaussia RLU/200 µl (A and B) and normalized by protein amount i.e. Gaussia RLU/µg protein (C and D). The yellow bar marks the activity of the inducer plasmid relevant for Notch pathway. Plotted data is averaged from three independent experiments (each with three replicates; *P< .05, **P< .01, ***P< .001, n.s.= not significant; Mann-Whitney U Test.). n = xy + stddev.

Figure 34 shows the induction of the Wnt pathway by the pAd inducer plasmid in HEK293T 3P-Luc cells in its non-normalized and normalized (by the corresponding protein amount) version for 10,000 cells seeded. The graph giving the non-normalized values 24 hours after transfection (Fig. 34A), as well as the graph giving the normalized values 48 hours after transfection (Fig. 34D) show a highly significant signal, but unfortunately for the cells treated with the control plasmid pUC19. In the non-

normalized read-out after 48 hours (Fig. 34B) and the normalized read-out after 24 hours (Fig. 34C) no Wnt induction was significantly detectable.

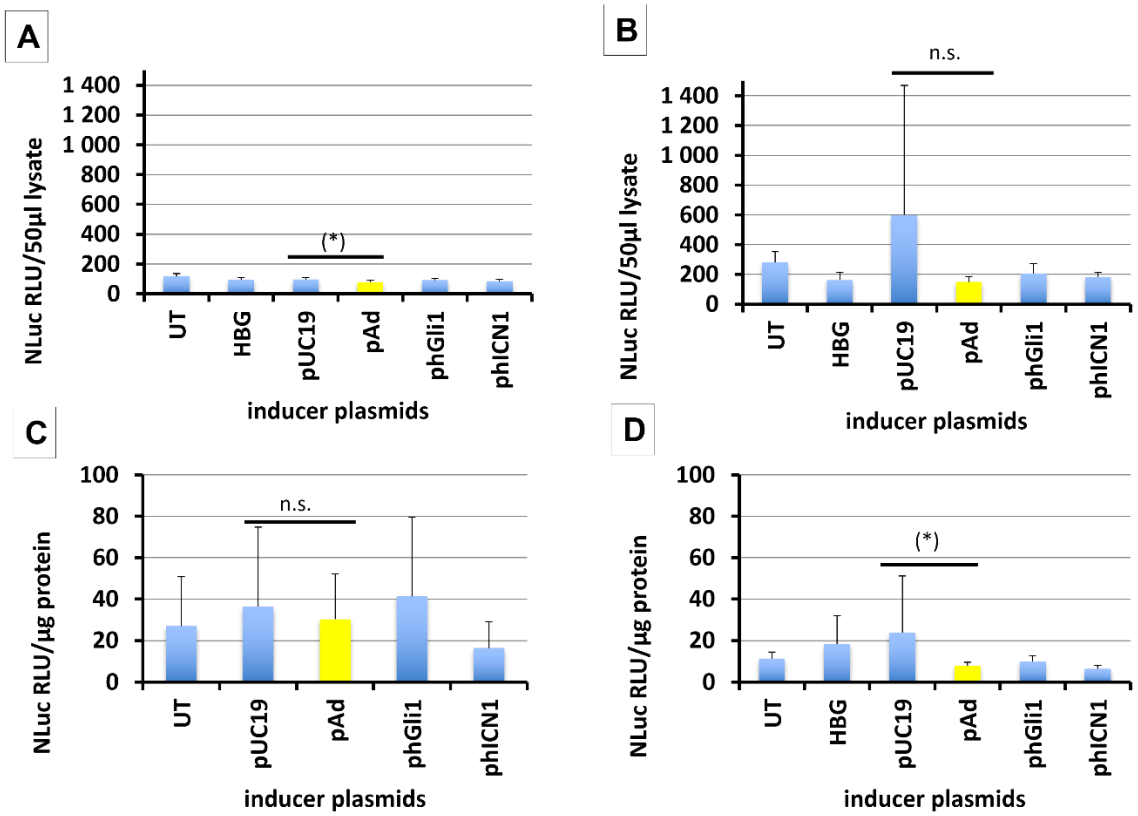

Figure 34: Wnt pathway activity estimation in HEK293T 3P-Luc cells (via NanoLuc read-out from Multi-Luc/BCA assay) after transfection with pathway-inducer plasmids. 10,000 cells were seeded for a day and then treated with different plasmid based polyplexes (pUC19-control plasmid; pAd-Wnt pathway inducer; phGli1-Hedgehog pathway inducer; phICN1-Notch pathway inducer) or HBG buffer or were left untreated (UT). Multi-Luc/BCA assay was performed by using the method without scratching 24h (A and C) or 48h (B and D) after transfection. NanoLuc expression is plotted as non-normalized i.e. NLuc RLU/50 µl (A and B) and normalized by protein amount i.e. NLuc RLU/µg protein (C and D). The yellow bar marks the activity of the inducer plasmid relevant for Wnt pathway. Plotted data is averaged from three independent experiments (each with three replicates; *P< .05, **P< .01, ***P< .001, n.s.= not significant; Mann-Whitney U Test.). n = xy + stddev.

Figures 35 images the induction of the Wnt pathway by the pAd inducer plasmid in HEK293T 3P-Luc cells in its non-normalized and normalized (by the corresponding protein amount) version for 20,000 cells seeded. Both non-normalized experiments 24 hours (Fig. 35A) and 48 hours after transfection (Fig. 35B), as well as the normalized

read-out 24 hours after transfection (Fig. 35C) show no significant pathway induction. In the normalized pathway read-out after 48 hours (Fig. 35D), even the cells treated with the control plasmid pUC19 give a significantly higher signal than the cells treated with pAd, the inducer plasmid.

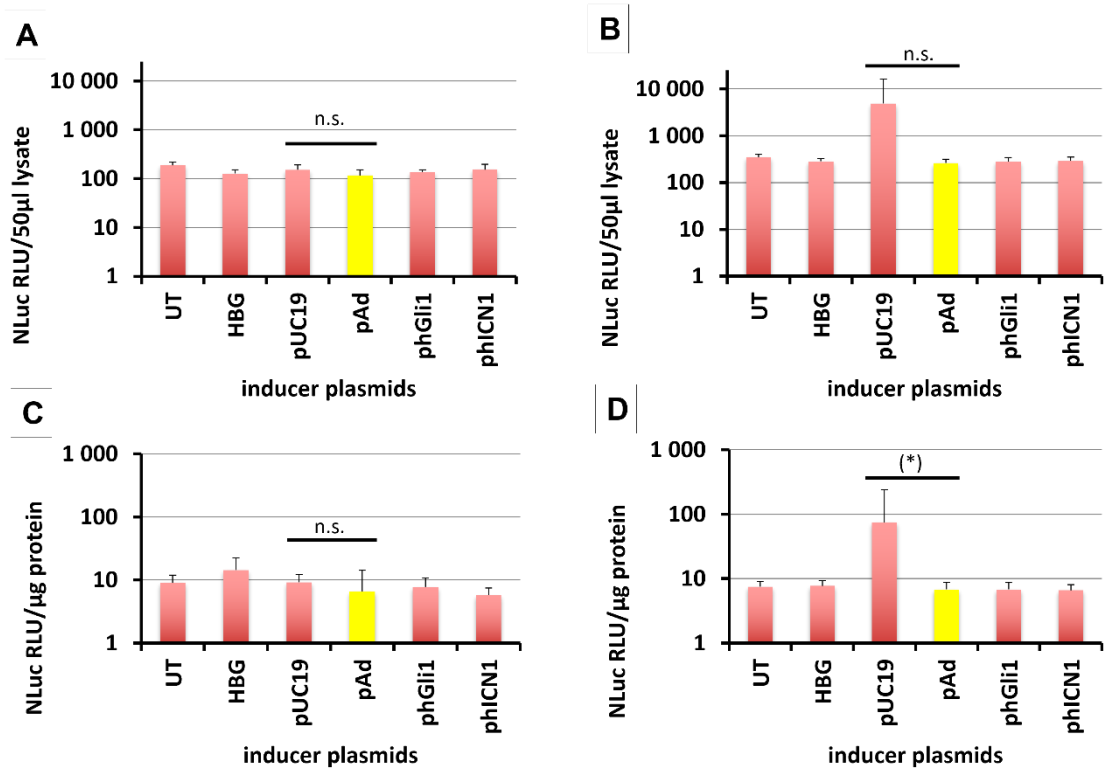

Figure 35: Wnt pathway activity estimation in HEK293T 3P-Luc cells (via NanoLuc read-out from Multi-Luc/BCA assay) after transfection with pathway-inducer plasmids. 20,000 cells were seeded for a day and then treated with different plasmid based polyplexes (pUC19-control plasmid; pAd-Wnt pathway inducer; phGli1-Hedgehog pathway inducer; phICN1-Notch pathway inducer) or HBG buffer or were left untreated (UT). Multi-Luc/BCA assay was performed by using the method without scratching 24h (A and C) or 48h (B and D) after transfection. NanoLuc expression is plotted as non-normalized i.e. NLuc RLU/50 µl (A and B) and normalized by protein amount i.e. NLuc RLU/µg protein (C and D). The yellow bar marks the activity of the inducer plasmid relevant for Wnt pathway. Plotted data is averaged from three independent experiments (each with three replicates; *P< .05, **P< .01, ***P< .001, n.s.= not significant; Mann-Whitney U Test.). n = xy + stddev.

To summarize all findings, it is striking that induction of any tested pathway was not statistically significant, when compared with pUC19 transfection control. In some cases, the measured activity of the pUC19-treated cells is even higher than the one of the cells

treated with the respective inducer plasmid. One possible explanation for the excessive pUC19 activity which blames the overspill from one well to another (particularly from a well treated with an inducer plasmid to another well only treated with the transfection control) during the scratching process has to be discarded in this case, since the process did not even include scratching the cell lysate from the surface. More likely, pUC19 might hold responsibility for its high activity as the used aliquot had already been opened before and maybe impaired in its function due to contamination or wrong storage conditions. Another possible reason might be that the amount of the inducer plasmids added (20 µg/ml; 200 ng/well) was potentially insufficient and therefore the activity of the inducer plasmids was too low for a successful detection. In this case, further experiments with different increased plasmid amounts added could be a promising approach. One of the main possible reasons for low induction signals concerns the small proportion of HEK293T 3P-Luc cells transduced with the multi-reporter plasmid and will be discussed in detail in the following section.

6.3. Characterization of HEK293T 3P-Luc Cells for EGFP Expression Using Fluorescence Microscopy and Flow Cytometry

As mentioned previously, HEK293T 3P-Luc cells were routinely characterized for EGFP expression by fluorescence microscopy every week. Alison Camungol, a former diploma student, handed the cells over with an EGFP-positive share of around 20% at the beginning of this project. The density of fluorescent cells here was only estimated in correlation to their cell density visible under phase contrast. According to the images obtained with the help of fluorescence microscopy (Figure 36), the cells seemed to become more fluorescent over time. Here, the incidence of cells emitting green fluorescence was estimated to be still around 20%.

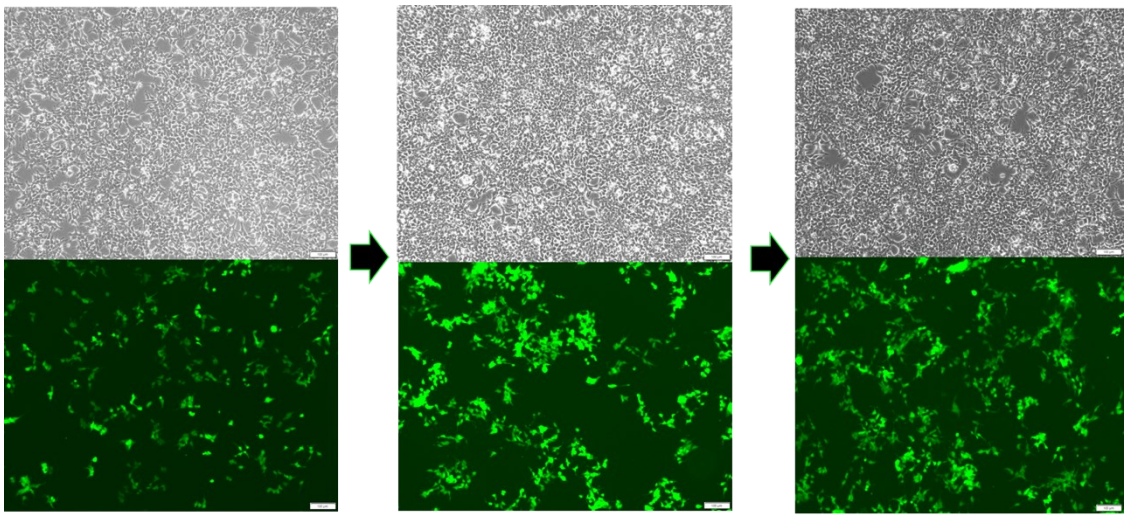

Figure 36: Fluorescence timeline of HEK293T 3P-Luc cells.
EGFP-positive cells are detected in application of the fluorescence microscope, visible in the pictures below. The pictures above display the corresponding cell densities visible under phase contrast, captured at the same position and scale, respectively. The dates plotted correspond with the date when the pictures were taken, the passaging number is plotted as P.x.

To confirm the estimated incidence of EGFP-positive HEK293T 3P-Luc cells, their fluorescence level was additionally checked with the FACS method once at the end of

this project. As mentioned above, the emitted fluorescence was detected in both HEK293T wt and 3P-Luc cells with two samples using the FITC channel. Via the *FlowJo* software (FlowJo™ Software, 2019) all cells of the same cell type were gated followed by gating only single cells. Out of this selection EGFP-positive and -negative cells were gated in one histogram and further separately displayed in single histograms, as it can be seen in the first row of Figure 37 which gives the gating strategy of HEK293T wt as an example. The comparison of histograms showing both EGFP-positive and -negative cells reveals an average proportion of 21.7% EGFP-positive cells in all HEK293T 3P-Luc detected. In other words, 21.7% of HEK293T 3P-Luc cells express the EGFP gene at the moment of the measurement and therefore harbor the 3P-Luc plasmid. As the FACS measurement has only been carried out once in duplets yet, more experiments are required to accurately prove this result.

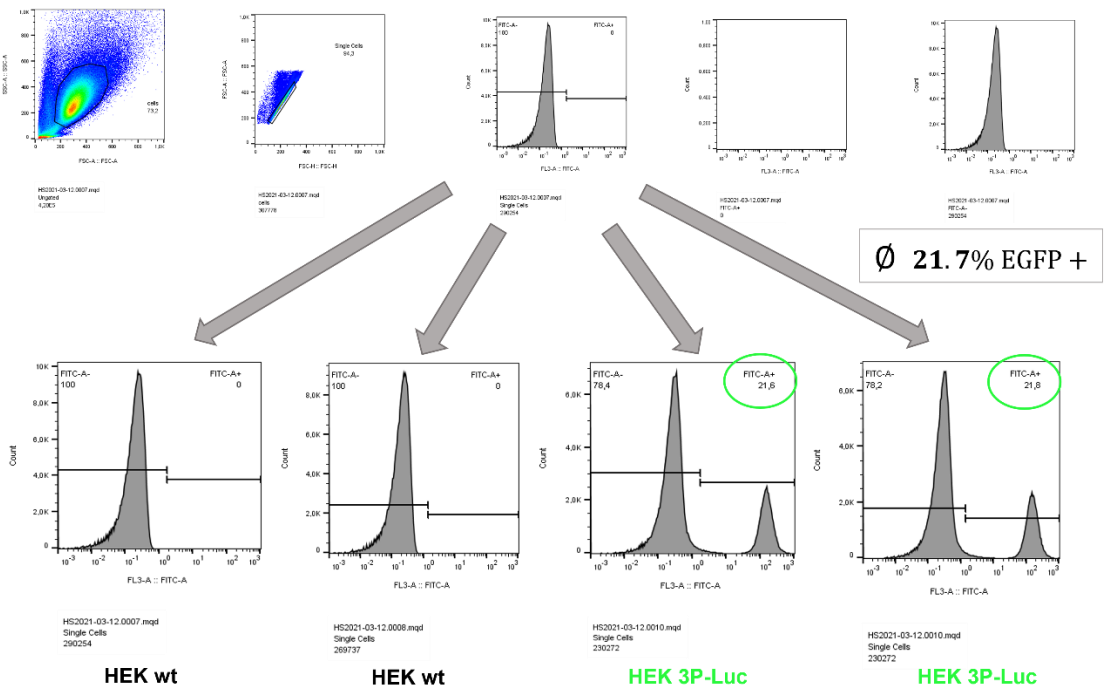

Figure 37: Representative gating strategy in HEK293T wt (P.67) and display of EGFP-positive HEK cells (HEK293T 3P-Luc (P.61)).

The first row shows the applied gating order after flow cytometry – here representative in HEK293T wt cells – detecting fluorescence (525/50 nm) applying the FITC channel. The second row illustrates all histograms including both EGFP-negative and -positive cells of all four samples. 21.7% on average of all measured HEK293T 3P-Luc cells express the EGFP gene. For analyzing the data derived from flow cytometry, the *FlowJo* software was used.

A possible explanation for the absence of signal pathway induction in HEK293T 3P-Luc may be the combination of the three following factors. At first, the amount of inducer plasmids used might have been insufficient, as already mentioned. Secondly, there is only a small proportion of HEK293T 3P-Luc cells successfully stably transduced with the 3P-Luc plasmid (21.7%). In other words, only 21.7% of all HEK293T 3P-Luc cells even had the ability to get transfected. At last, the inducer plasmids themselves have a transfection efficiency in the range of 10-20%. Which means, out of the 21.7% of all HEK293T 3P-Luc cells, only 10-20% actually were transfected by the inducer plasmids. This combination may result in very low induction signals of the tested cells. Cell sorting of the HEK293T 3P-Luc cells and, thus, increasing the proportion of HEK293T 3P-Luc cells containing the multi-reporter plasmid among all supposed HEK293T 3P-Luc cells, is required before conducting further experiments with this approach in the future. Another additional option might be using higher amounts of inducer plasmids in the future.

7. Conclusion

In current biomedical research, multiple embryonic signal transduction pathways associated with carcinogenesis and chemoresistance in CSC are of high interest.

The thesis focuses on characterizing HEK293T 3P-Luc cells for Sonic Hedgehog, Notch and Wnt pathway activity, since several studies haven proven them to be linked with tumorigenesis and the control of CSC, which are responsible for tumor relapse and malignancy. This was performed via Multi-Luc/BCA assay.

According to our findings, the protein amounts of HEK293T 3P-Luc cells (as compared to HEK293T wt cells) determined by the Multi-Luc/BCA assay are poor and not as expected. However, it is evident that after both incubation durations tested the alternative method without scratching, on the one hand, leads to both higher and more appropriate protein amounts in total compared to the common method with scratching. On the other hand, the method without scratching also yields a higher proportionality attended by a higher accuracy of the rising HEK293T 3P-Luc values in comparison to the alternative method.
These poor protein amounts and normalized signal values definitely pose a limitation to this work. Possibly they are caused by the potential overspill or even partly loss of cell lysate while scratching or in the case of the alternative method, incomplete lysis of the cells. For further experiments using scratching, the physical separation of wells might help, but would require a higher number of well plates.

Taken together, the Sonic Hedgehog pathway activity is not significantly detectable, except for one experiment. With applying the method including scratching after an incubation time of 48 hours, we were able to slightly detect the Hedgehog in HEK293T 3P-Luc cells.
In contrast to this, the Notch activity is highly significantly detectable in HEK293T 3P-Luc cells and increases proportionally to the cell count in both methods used and after both incubation durations tested.

For both techniques used, the Wnt pathway activity is not properly detectable 24 hours after seeding, but significantly detectable after an incubation time of 48 hours. Applying the alternative method, the pathway activity increases more proportionally to the cell number and is considerably higher, in all. A possible reason for the irregular results and the absence of a rise proportional to the cell number with the method with scratching may be the scratching part itself and the difficulties coming along with it.

It is evident that induction of any signal pathway was not detectable in a statistically significantly manner, so the responsiveness of all measured pathways in HEK293T 3P-Luc cells for pathway modulators could not be proven within this work. On this account, further studies with alternative increased plasmid amounts on the one hand and cell sorting on the other hand ought to be performed to increase and determine the induction capability of the cells in question precisely.

8. List of Figures

9. References

Addgene. (n.d.). hGli1 flag3x. Retrieved from https://www.addgene.org/84922/.

Beyond Your Back Door. (2020). Are They Blinking Out? Retrieved from https://beyondyourbackdoor.net/2020/07/23/are-they-blinking-out/.

Braune, E.B., Lendahl, U. (2016). Notch -- a goldilocks signaling pathway in disease and cancer therapy. *Discovery Medicine*.

Brown, R.B., Audet, J. (2008). Current techniques for single-cell lysis. *J R Soc Interface*.

Carballo, G. B., Honorato, J. R., de Lopes, G., & Spohr, T. (2018). A highlight on Sonic hedgehog pathway. *Cell communication and signaling*.

Chopra, A. (2008) Gaussia princeps luciferase. *Molecular Imaging and Contrast Agent Database (MICAD)*.

England, C. G., Ehlerding, E. B., & Cai, W. (2016). NanoLuc: A Small Luciferase Is Brightening Up the Field of Bioluminescence. *Bioconjugate chemistry*.

FlowJo™ Software. (2019) (when applicable add—for Windows or for Mac) [software application] Version 10.7. Ashland, OR: Becton, Dickinson and Company.

Gibbons, A. E., Luker, K. E., & Luker, G. D. (2018). Dual Reporter Bioluminescence Imaging with NanoLuc and Firefly Luciferase. *Methods in molecular biology*.

Gruber, D. (2021). Optimization of firefly luciferase assay in spheroid cell culture models.

Hall, M. P., Unch, J., Binkowski, B. F., Valley, M. P., Butler, B. L., Wood, M. G., …, Wood, K. V. (2012). Engineered luciferase reporter from a deep sea shrimp utilizing a novel imidazopyrazinone substrate. ACS chemical biology.

Hooper, K. (2011). Multiplexing Cell-Based Assays: Get More Biologically Relevant Data. Retrieved from https://at.promega.com/resources/pubhub/multiplexing-cell-based-assays-get-more-biologically-relevant-data/#introduction-264b06c7-bdd3-4ce8-bb1a-a2353f269a6c.

JungleDragon. (n.d.). Deep water shrimp (Oplophorus gracilirostris) as it secretes a cloud of bioluminescent fluid as a defensive mechanism. Retrieved from https://www.jungledragon.com.

Komiya, Y., & Habas, R. (2008). Wnt signal transduction pathways. *Organogenesis*.

Lee, J. (2008). Bioluminescence: the First 3000 Years. *Biology.3*.

Li, X., Ortiz, M. A., & Kotula, L. (2020). The physiological role of Wnt pathway in normal development and cancer. *Experimental biology and medicine (Maywood, N.J.)*.

Luo, Q., Kang, Q., Si, W., Jiang, W., Park, J.K., & Peng, Y, …, He, T.C. (2004). Connective tissue growth factor (CTGF) is regulated by Wnt and bone morphogenetic proteins signaling in osteoblast differentiation of mesenchymal stem cells. *J Biol Chem*.

Maier, J., Elmenofi, S., Taschauer, A., Anton, M., Sami, H., & Ogris, M. (2019). Luminescent and fluorescent triple reporter plasmid constructs for Wnt, Hedgehog and Notch pathway. *Plos One*.

Man, T. P. (2019). G-Biosciences. Retrieved from https://info.gbiosciences.com/blog/luciferase-reporter-assays.

Marques, S.M., Esteves da Silva, J.C. (2009). Firefly bioluminescence: a mechanistic approach of luciferase catalyzed reactions. *IUBMB Life*.

Norrander, J., Kempe, T., & Messing, J. (1983). Construction of improved M13 vectors using oligodeoxynucleotide-directed mutagenesis. *Gene*.

Promega. (n.d.). Luciferase Assay System Technical Bulletin. Retrieved from https://at.promega.com/resources/protocols/technical-bulletins/0/luciferase-assay-system-protocol/.

Promega. (n.d.). Passive Lysis 5X Buffer. Retrieved from https://at.promega.com/products/luciferase-assays/reporter-assays/passive-lysis-5x-buffer/?catNum=E1941#specifications.

Promega. (n.d.). Technical Manual. Nano-Glo® Luciferase Assay System. Instructions for Use of Products. N1110, N1120, N1130 and. N1150. Retrieved from https://at.promega.com/-/media/files/resources/protocols/technical-manuals/101/nanoglo-luciferase-assay-system-protocol.pdf?rev=996b868511724a55b1eeeb6c3cc0ab3b&sc_lang=en.

Roberts, R. (2020). What the HEK? A Beginner's Guide to HEK293 Cells. Retrieved from https://bitesizebio.com/45489/what-the-hek-a-beginners-guide-to-hek293-cells/.

Sarrion-Perdigones, A., Chang, L., Gonzalez, Y., Gallego-Flores, T., Young, D. W., & Venken, K. (2019). Examining multiple cellular pathways at once using multiplex hextuple luciferase assaying. *Nature communications*.

Sever, R., & Brugge, J. S. (2015). Signal transduction in cancer. *Cold Spring Harbor perspectives in medicine*.

Siebel, C., & Lendahl, U. (2017). Notch Signaling in Development, Tissue Homeostasis, and Disease. *Physiological Reviews*.

Sigma Aldrich. (n.d.). Bioluminescent Firefly Luciferase Assays. Retrieved from https://www.sigmaaldrich.com/technical-documents/articles/biology/cell-culture/firefly-luciferase-assays.html.

Sigma Aldrich. (n.d.). G 418-disulfat (Salz)-Lösung. Retrieved from https://www.sigmaaldrich.com/catalog/product/sigma/g8168?lang=de&region=AT&gclid=EAIaIQobChMIirW6n_a38AIV1OFRCh1qow6tEAAYASAAEgKaRPD_BwE.

Skoda, A. M., Simovic, D., Karin, V., Kardum, V., Vranic, S., & Serman, L. (2018). The role of the Hedgehog signaling pathway in cancer: A comprehensive review. *Bosnian journal of basic medical sciences*.

Statistics, S. S. (2021). Retrieved from https://www.socscistatistics.com.

Takebe, N., Miele, L., Harris, P. J., Jeong, W., Bando, H., Kahn, M., . . . Ivy, S. P. (2015). Targeting Notch, Hedgehog, and Wnt pathways in cancer stem cells: clinical update. *Nature Reviews Clinical Oncology*.

Taschauer, A., Geyer, A., Gehrig, S., Maier, J., Sami, H., & Ogris, M. (2016). Upscaled synthesis and characterization of nonviral gene delivery particles for transient in vitro and in vivo transgene expression. *Hum Gene Ther Methods*.

The Y.O.R.F. (2007) Bioluminescence. Retrieved from http://theyorf.blogspot.com/2007/09/bioluminescence.html.

Thermo Fisher Scientific. (n.d.). Cell Lysis Solutions. Retrieved from https://www.thermofisher.com/at/en/home/life-science/protein-biology/protein-biology-learning-center/protein-biology-resource-library/pierce-protein-methods/cell-lysis-solutions.html.

Thermo Fisher Scientific. (n.d.). Gaussia Luciferase Assays & Vectors. Retrieved from https://www.thermofisher.com/at/en/home/life-science/protein-biology/protein-assays-analysis/reporter-gene-assays/luciferase-assays/gaussia-luciferase-assays-vectors.html.

Thermo Fisher Scientific. (n.d.). Overview of Cell Lysis and Protein Extraction. Retrieved from https://www.thermofisher.com/at/en/home/life-science/protein-biology/protein-biology-learning-center/protein-biology-resource-library/pierce-protein-methods/overview-cell-lysis-and-protein-extraction.html.

Thermo Fisher Scientific. (2020). Pierce™ BCA Protein Assay Kit.

Thermo Fisher Scientific. (2020). Pierce™ Firefly Luciferase Glow Assay Kit.

Thermo Fisher Scientific. (n.d.). Reporter Gene Assays. Retrieved from https://www.thermofisher.com/at/en/home/references/gibco-cell-culture-basics/transfection-basics/reporter-gene-assays.html?gclid=EAIaIQobChMI5amzg6Gf8AIVTuqyCh2V6wUCEAAYASAAEgJ4XPD_BwE&ef_id=EAIaIQobChMI5amzg6Gf8AIVTuqyCh2V6wUCEAAYASAAEgJ4XPD_BwE:G:s&s_kwcid=AL!3652!3!305473461759!b!!g!!&cid=bid_clb_tfx_r01_co_cp0000_pjt0000_bid00000_0se_gaw_dy_pur_con&s_kwcid=AL!3652!3!305473461759!b!!g!!.

Thermo Fisher Scientific. (n.d.). Traditional Methods of Cell Lysis. Retrieved from https://www.thermofisher.com/at/en/home/life-science/protein-biology/protein-biology-learning-center/protein-biology-resource-library/pierce-protein-methods/traditional-methods-cell-lysis.html.

Thomas, P. & Smart, T. (2005). HEK293 cell line: A vehicle for the expression of recombinant proteins. *Journal of Pharmacological and Toxicological Methods*.

Weiss, S. (2020). Optimization of multi-reporter luciferase assays for simultaneous measurement of signaling pathway activities.

Wrobel, D. (n.d.). Midwater Copepod - 2. Retrieved from https://www.wrobelphoto.com/deepseamarinelife/hc92e6c2#hc92e6c2

Yu, T., Laird, J. R., Prescher, J. A., & Thorpe, C. (2018). Gaussia princeps luciferase: a bioluminescent substrate for oxidative protein folding. *Protein science: a publication of the Protein Society*.

10. Appendix

Normalized data

Figure 38 displays the normalized Notch pathway read-out by the Multi-Luc/BCA assay in HEK293T wt and 3P-Luc cells for the common method including scratching (Fig. 38A and 38B) and the alternative method without scratching (Fig. 38C and 38D) after an incubation time of 24 hours (Fig. 38A and 38C) and 48 hours (Fig. 38B and 38D). As described above, only positive values are displayed in the graphs given.

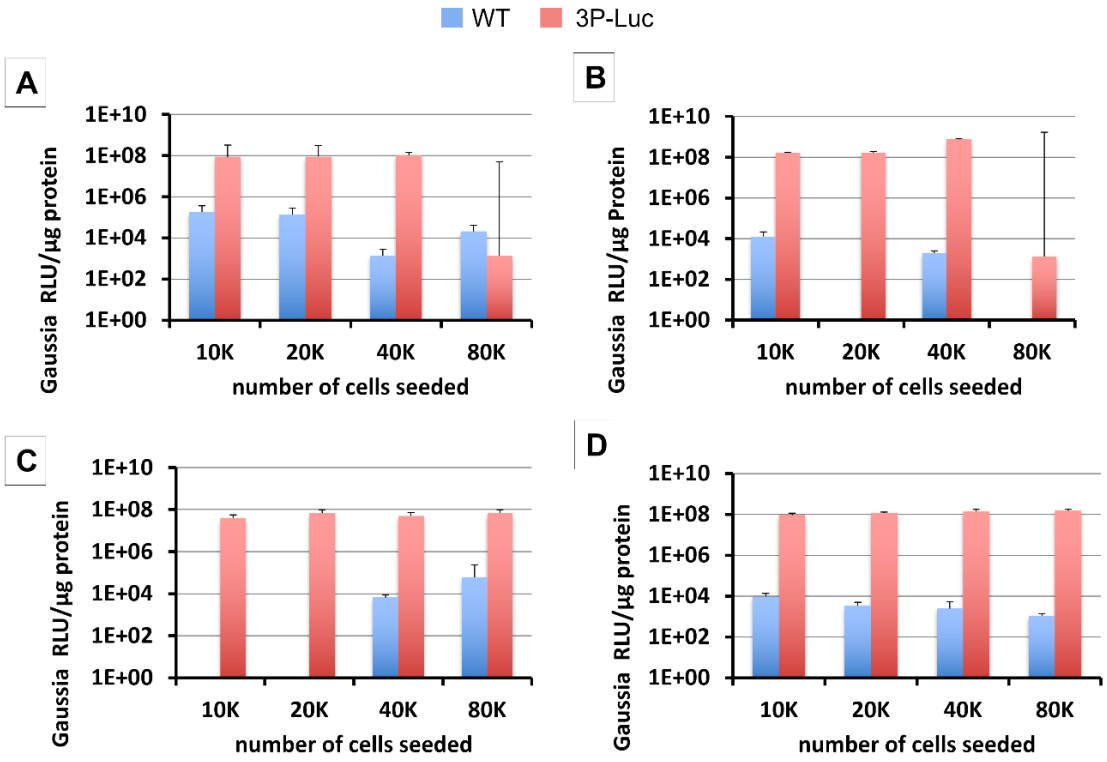

Figure 38: Normalized Notch pathway activity estimation in HEK293T 3P-Luc cells (as compared to HEK293T wt cells) via Gaussia luciferase read-out from Multi-Luc/BCA assay. Different numbers of cells per well were seeded and the Multi-Luc/BCA assay was performed by using the method with scratching (A and B) or without scratching (C and D). Gaussia luciferase expression data normalized by protein i.e. RLU/µg protein after 24h (A and C) or 48h (B and D) is plotted as average from three independent experiments. n = xy + stddev.

Figure 39 shows the normalized Wnt pathway read-out by the Multi-Luc/BCA assay in HEK293T wt and 3P-Luc cells for the common method including scratching (Fig. 39A and 39B) and the alternative method without scratching (Fig. 39C and 39D) after an incubation time of 24 hours (Fig. 39A and 39C) and 48 hours (Fig. 39B and 39D). As described above, only positive values are displayed in the graphs given.

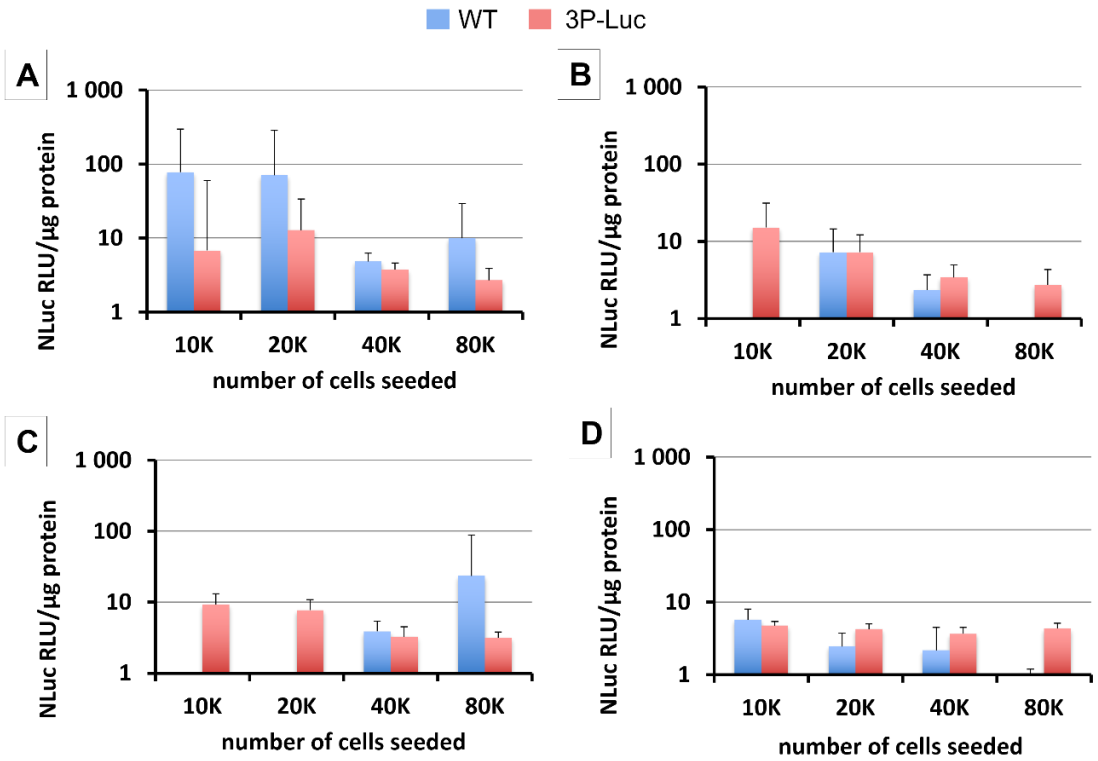

Figure 39: Normalized Wnt pathway activity estimation in HEK293T 3P-Luc cells (as compared to HEK293T wt cells) via NanoLuc read-out from Multi-Luc/BCA assay. Different numbers of cells per well were seeded and the Multi-Luc/BCA assay was performed by using the method with scratching (A and B) or without scratching (C and D). NanoLuc expression data normalized by protein i.e. RLU/µg protein after 24h (A and C) or 48h (B and D) is plotted as average from three independent experiments. n = xy + stddev.

It is evident, that the normalized pathway signals of both the Notch and the Wnt pathway are very irregular, some of them even in the negative area, and therefore not applicable. Obviously, the normalized Notch activity values are stronger and more appropriate than the signals indicating the Wnt activity. However, the normalized Notch signals also give negative values for the wt cell signals in some cases and cannot be

further used. A possible explanation for the superiority of the normalized Gaussia Luc assay results towards the normalized NanoLuc assay results might be the omission of the scratching and lysing part and all issues linked to them in the Notch read-out.